

MDT Wiring at CERN

CERN/Geneva

W. Flegel, C. Rosset, F. Cataneo, R. Dumps, D. Rotil, F. Rosset, F. Linde, R. Lindner,
M. Spegel, W. Riegler, J. Wotschack, C. Fabjan, M. Treichel, G. Lion

INFN/Frascati

B. Esposito, M. Curatolo, M. Spitalieri, P. Benvenuto, C. Capoccia, A. Ceccarecci

NIKHEF/Amsterdam

A. Colijn, E. Visser, M. Woudstra, P. Werneke, A. Korporaal, H. van der Graaf,
G. Massaro, W. Gootink, G. Bobbink

Brandeis University/Boston

H. Wellenstein

1 Introduction

The Monitored Drift Tubes (MDTs) for the BOL and BML prototypes of the ATLAS muon spectrometer require¹ in addition to the wire locators at the tube ends a wire locator at the tube centre. This is why we wired these MDTs at the 'CERN robot' which was originally developed for the production of High Pressure Drift Tubes with many intermediate wire locators.

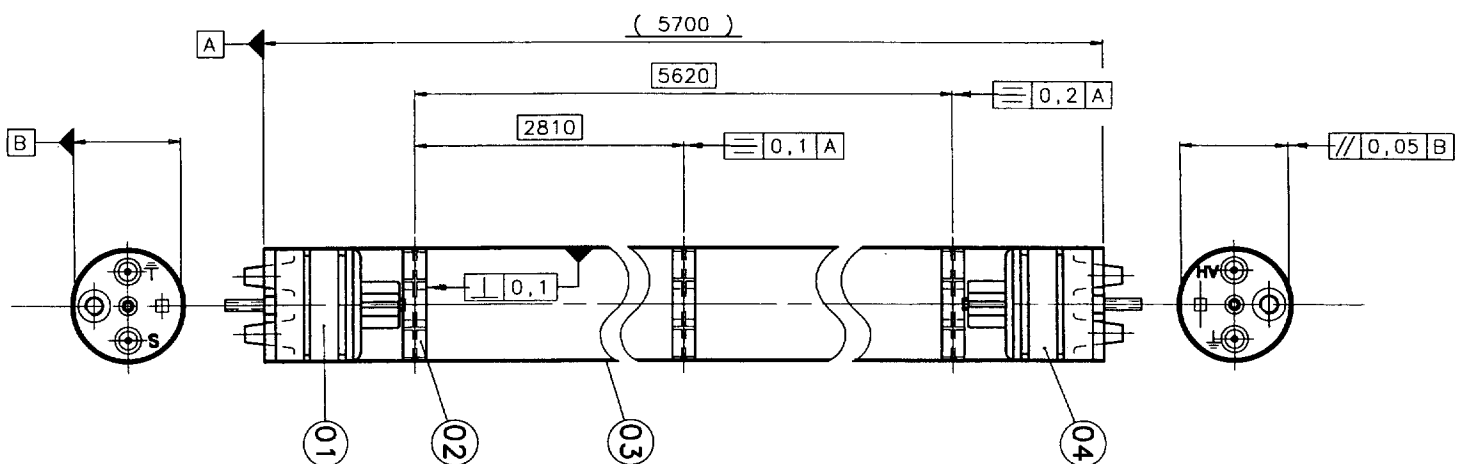


Figure 1: Engineering drawing of a long MDT for the BOL prototype.

¹At least this is the assumption at this moment; in the near future the need for a central locator must (and will) be examined in depth!

In this note we report on the MDT components (tubes, wire, locators and end-plugs), on the MDT assembly and on the quality control of a completed MDT. An engineering drawing of a long MDT for the BOL chamber is shown in Figure 1. In addition to the component locations, also the relative orientation of the two end-plugs and the tube length are important in view of the hedgehog electronics mount. A video of the wiring process is available as well at CERN.

2 Components: Tube, Wire, Locator and End-plug

2.1 Tube

For the BOL MDT chamber we used tubes manufactured by Menziken/Switzerland. From metrology measurements on a small sample of short tubes we find the characteristics as listed in Table 1. The company delivered 700 tubes cut to a length of 5700 mm, deburred and pre-cleaned. To allow for light paths for the alignment monitors, 45 of these tubes were re-cut at CERN to a length of 5180 mm. Subsequently all tubes were cleaned at CERN prior to wiring. The cleaning included: (1) pre-cleaning in per-chlorine ethylene vapour, (2) washing under ultrasonic vibrations in an alkaline (pH=10) bath (Henkel P3-ALMECO 18), (3) rinsing with demineralized water, (4) drying with nitrogen and (5) cooking at 150 °C. Before boxing the cleaned tubes, the two tube ends were wrapped in aluminium foil to protect the inside from dust and other undesired animals.

Parameter	Menziken Tubes	Metalba Tubes	MDT Specification
Outer Diameter	29.982 ± 0.003 mm	29.988 ± 0.003 mm	$30.000^{+0}_{-0.030}$ mm
Inner Diameter	29.187 ± 0.004 mm	29.178 ± 0.002 mm	-
Wall thickness	398 ± 6 μ m	405 ± 6 μ m	400 ± 20 μ m
Eccentricity	≈ 10 μ m	≈ 10 μ m	< 16 μ m
Ellipticity	≈ 10 μ m	≈ 10 μ m	-
Straightness	—	—	30 μ m / 30 cm

Table 1: Tube specifications and the metrology results for Menziken and Metalba tubes. Eccentricity is half the difference between the maximal and the minimal wall thickness. Ellipticity is half the difference between the long axis (≥ 30.000 mm) and the short axis (≤ 30.000 mm) found fitting an ellipse to a set of measured points along the tube outer diameter.

The tubes for the BML chamber came from Metalba/Italy. The characteristics, again measured on a small sample of short tubes, are also listed in Table 1. Metalba delivered 4005 mm and 4700 mm long tubes, not deburred and not cleaned at the factory. These tubes underwent the same cleaning process as the BOL tubes. After the cleaning process we still had to cut the long 4700 mm tubes either to the required length for ‘long’ BML tubes (4005 mm) or to the required length for ‘short’ BML tubes (3460 mm). Also, as opposed to the BOL tubes, all BML tubes, i.e. also those already cut by Metalba to the correct 4005 mm length, had to be deburred. Naturally, in the future re-cutting and/or deburring ought to be done prior to cleaning the tubes.

From Table 1 we conclude that both the tubes delivered by Menziken and the tubes delivered by Metalba meet the required MDT specifications listed in the same table.

2.2 Wire

We used 50 μm diameter W-Rh (97/3) gold-plated (3% by weight) wire from Luma/Sweden as well as from Sylvania/USA. Small samples of the Luma wire were inspected for defects, wire diameter and wire elongation as a function of the applied force. An example is shown in Figure 2. From these measurements we concluded that the wire diameter

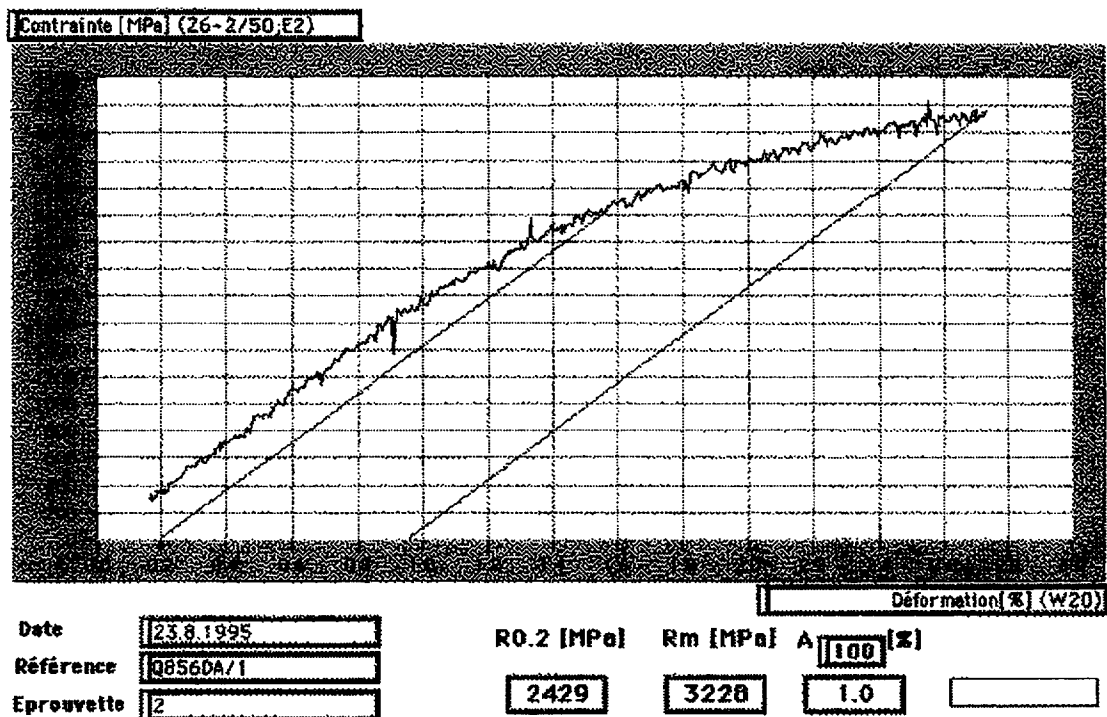


Figure 2: *Elongation of a sample of Luma wire as a function of the applied force. Apart from the measurement, two parallel lines are indicated. These are standard ways to specify the elastic limit and the rupture limit. For this particular sample the rupture limit (called 'Rm') was determined to be 3228 MPa. This corresponds to 620 grams. As an aside, this same figures also shows that in the elastic regime, the wire elongation is about: 3×10^{-5} /gram. This is used as input for our temperature correction of the measured wire tension as discussed in Section 4.2.*

met the requested specification². We also determined the rupture limit to be 620 grams. Initially we decided to wire the BOL (and BML) tubes at 380 grams. However, due to problems with the wire crimp, we lowered the tension to 250 grams for the BOL tubes and 300 grams for the BML tubes. With hindsight, we probably should have wired all tubes at the initially planned 380 grams.

²The systematic uncertainty in the measurement of the wire diameter is about 2 μm . Systematic changes of up to 2% in the wire tension of BML tubes after changing from one spool of wire to another suggest that the wire diameter is precise to within 0.5 μm . This is consistent with the 1% tolerance on the wire diameter stated by the manufacturer.

As an aside: we always measured the wire resistance immediately after a tube was produced. This to check for wire ruptures. In these tests we also noticed percent level jumps in the measured resistance in going from one spool to another. This again indicates that on the percent level wire parameters (probably the wire diameter) are changing.

2.3 Locator

Two wire locators were used; a locator designed at CERN and produced by Wüst in Germany (Bavaria for insiders as we understand!) and a locator designed by Frascati and produced by LMP in Italy. In the sequel we will refer to these locators as the ‘German’ one and the ‘Italian’ one, respectively. These locators are shown in Figures 4 and 5 respectively, together with the XY coordinate frame used by us in e.g. the wire location analysis. In Figure 3 we show a blown-up view of the wire localising region. This figure is for the German locator design with a $50 \times 50 \mu\text{m}^2$ central square hole for the wire. For the Italian locator the design size of the square was slightly larger: $51 - 61 \times 51 - 61 \mu\text{m}^2$. At the centre position of the tubes we *always* used a German locator; at the tube ends we used German locators as well as Italian locators.

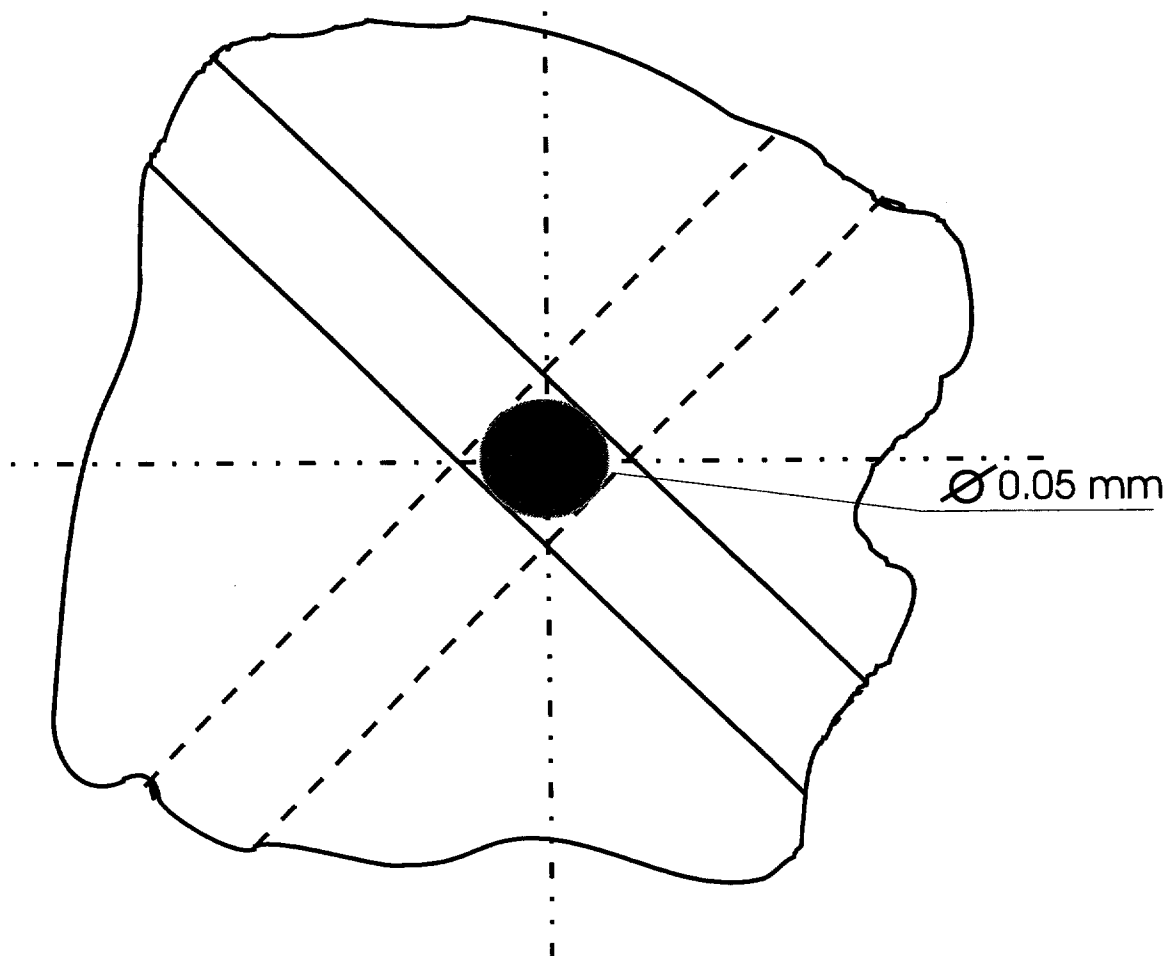


Figure 3: *The wire as localised in a perfect wire locator. The German locator has by design a $50 \times 50 \mu\text{m}^2$ square in the central region and the Italian locator has by design a $51 - 61 \times 51 - 61 \mu\text{m}^2$ square in the central region.*

2.3.1 'German' locator

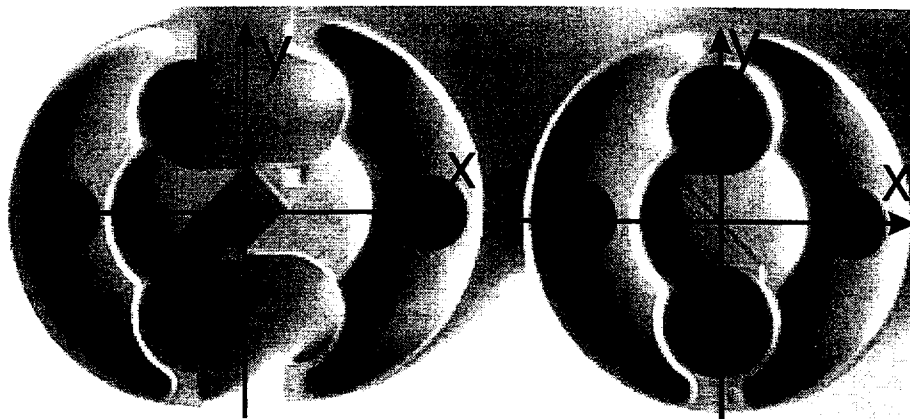


Figure 4: *The German wire locator* The basic half-locators are shown as well as an assembled locator.

The German locator consists of two symmetric (identical!) halves which click together to form a single inseparable unit (see Figure 4). The material is Vectra, a glass-fibre loaded plastic. In the other view (not shown in this figure, but visible in Figure 11), the locator is 6 mm wide and it has a small groove at the center. By design the locator is slightly smaller than the inner diameter of the tubes, 29.200 mm for the tube compared to 29.150 mm for the locator. This ideally left a 25 μm between the locator and the inner tube wall. However, since the tolerance on the tube outer diameter is asymmetric, the companies aimed for an averaged outer diameter of 29.985 mm instead of the advocated 30.000 mm. This reduces the design gap between locator and tube to an uncomfortably small 18 μm . The small groove on the outer rim of the locator is used to fix this locator in position by slightly denting the tube in the correct location. After some tests with mechanical crimps we decided to realize the concentric indentation of the aluminium tube with the air-pressure crimper developed by our Frascati colleagues. We used a pressure of 140 Bars to realize this crimp. A picture of this crimp, and the crimp on the end-plug, can be seen in Figure 6. The main reason we opted for the air-pressure crimp is that, as opposed to our first mechanical crimps, the air-pressure crimp *only* deforms, dents, the aluminium tube to the inside. I.e. it does *not* introduce any noticeable upward bumps on the aluminium tube. This is very important for the subsequent stacking of tubes, since it is precisely the wire locator region where we aim for the largest precision! A disadvantage, at least for some tube stacking schemes, is that the air-pressure crimp, despite the small (about 2 mm width of the O-ring used to transfer the force onto the tube, leads to a deformation which extends along the length of the tube for more than 20 mm. This requires that during tube stacking the tubes ought to be held over a longer length. We also verified that even in the region of the locator crimp, the vacuum suction heads, used by several tube assembly method as a way to force the tubes into the jigging, still make good contact to the tube in the important wire locator crimp region.

Because of the symmetry the center of the central hole is always at the tube axis. Its shape, however, can deviate from the design shape of a $50 \times 50 \mu\text{m}^2$ square (a bit small to our taste, but ...). Metrology measurements indeed indicated defects in the design as well as in the realisation of this locator:

- central hole: the size and the shape of the central hole depend on the force used to click the two halves together. It varies from as large as $80 \times 140 \mu\text{m}^2$ to as small, but still too large, as $80 \times 60 \mu\text{m}^2$.
- shape: The assembled locator is slightly elliptical. It measures typically 29.050 mm in the X direction and 29.150 mm in the Y direction (see Figure 4). The design value was 29.150 mm. This shape of the locator is transferred to the shape of the tube which in turn will impact on the stacking precision *unless* the locators are all mounted identically within the tubes. (We tried to do this.)
- clicking mechanism: By design the mounting of the two halves left an ambiguity in the relative location of the two halves in the Y direction (see Figure 4). This should be improved upon in a future production run if we decide to proceed with this locator.

The company has been informed of the defects and has been asked to improve them. In view of time constraints we decided to wire both the BOL and BML tubes with the first batch of wire locators. The same metrology measurements also indicated an excellent wire localising capability of this locator of about $10 \mu\text{m}$ w.r.t. the tube (i.e. $10/\sqrt{2} \approx 7 \mu\text{m}$ in one direction). Here it should be noted that of the 6 tube-locator assemblies, only 5 could be measured. In the sixth the central hole in the wire locator was invisible! The quoted $10 \mu\text{m}$ gives the deviation in space between the centre of the square hole in the wire locator and the centre of the circle fitted to measurements on the outer tube wall. Therefore this $10 \mu\text{m}$ does *not* take into account additional wire location uncertainties due to the too large size of the central square.

To avoid contributions to the wire location from the locator's ellipticity, we mounted most locators in a well defined orientation within the tube. We also always used the same, 140 Bar, force to finally mount the two half-locators together (of course the two half locators are clicked together manually and only later the 140 Bar air-pressure crimp is exerted).

2.3.2 'Italian' locator

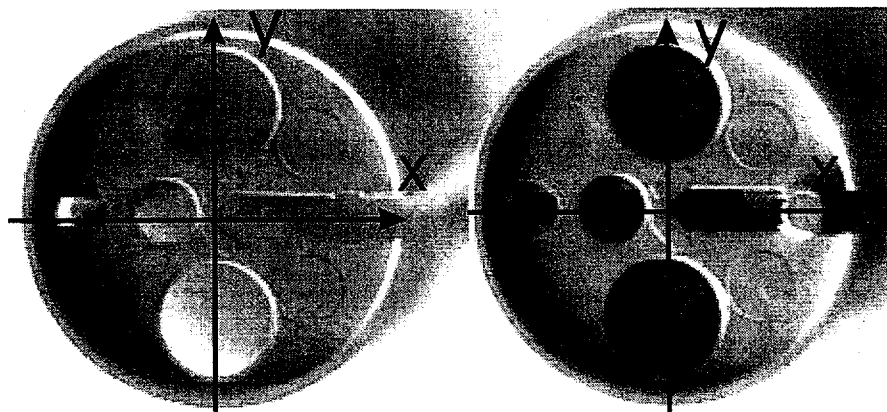


Figure 5: *The Italian wire locator. Its basic half-locator is shown as well as an assembled locator.*

Also the Italian locator consists of two symmetric (identical!) halves which together form a single unit. The material is Noryl, another glass-fibre loaded plastic. Some Italian locators were white and others were black, this is supposed to be irrelevant. Contrary to the German locator, an assembled Italian locator can be taken apart again. As is evident from Figure 5 the Italian locator separates exactly in the other plane as the German locator. This made the production in view of the required precision much simpler. It however, makes the sliding of the locator within a tube less predictable. Also the Italian locator can not be crimped upon to fix its position inside a tube. Therefore the Italian locators are ‘slightly’ oversized, $29.20^{+0.02}_{-0.00}$ mm compared to the 29.200 mm inner tube wall diameter. At CERN we did not perform separate metrology measurements on Italian locators. In Frascati they did investigate the wire localising capabilities of this locator (9 samples). In summary they found that the Italian locator positions a wire with an r.m.s. precision of about $15 \mu\text{m}$ within a tube (i.e. $15/\sqrt{2} \approx 11 \mu\text{m}$ in one direction).

2.4 End-plug

All tubes were wired using the Frascati end-plug. The basic end-plug material is Noryl. The end-plug consists of two mold injected parts, an aluminium ring for the ground contact, a copper tube for the wire fixation, electrical components like capacitor and resistor, potting material and pins for the connection to the pre-amplifiers/high voltage and gas manifold. The critical dimension regarding our wiring scheme are the outer diameter of the plastic pieces: 29.1 mm and the outer diameter of the aluminium ring: 28.9 mm (both should be compared to the inner diameter of the aluminium tubes of 29.200 mm). So on paper there is sufficient clearance between end-plug diameter and tube inner wall. In reality the clearance did exist as well, but from time to time less than the expected 0.1 mm due to skewed assembly of the plastic pieces and the aluminium ring.

Prior to the start of the BOL and BML production, the original end-plug underwent some modifications to (1) make the wire crimp possible, (2) allow the mounting of the hedgehog printed circuit boards and (3) to use the air pressure crimp for the fixation of the end-plug at the tube ends. The details of this Frascati end-plug are available in a separate note. A photo of this end-plug as used by us is shown in Figure 6. Before shipment to CERN, these end-plugs are inspected visually for defects and for HV (leak current) in Frascati. Upon arrival at CERN, the end-plugs are inspected for leaks prior to wiring.

During the wiring process two actions are required on the end-plug: (1) the end-plug must be crimped into the tube to withstand the mechanical forces due to the overpressure of 2 Bars (and much more in view of safety!) and (2) the W-Rh wire must be crimped, after tensioning to the required tension, into the 2 mm (inner) diameter Indium dipped copper tube mounted in the center of the end-plug (see Figure 6). We finally opted for the simple air-pressure crimp developed by our Frascati colleagues for the fixation of the end-plug. We typically employed a pressure of 185 – 200 Bars to dent the aluminium tube into the O-ring groove on the end-plug. The result after this crimp is shown in Figure 6 as well. For the wire fixation we used a mechanical crimp to deform the copper tube into the shape shown in Figure 7. Compared to a simple flattening of the copper tube, this particular C-shape crimp has the advantage that the wire is held much better, provided

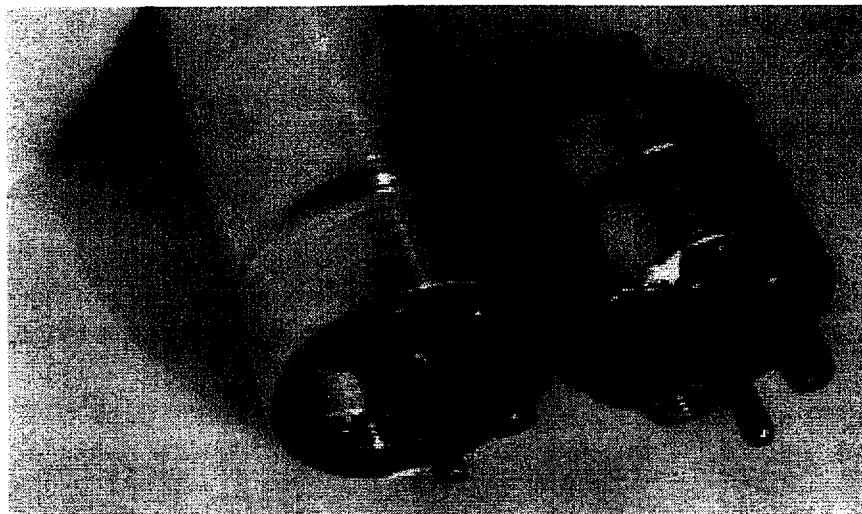


Figure 6: (a) The Frascati end-plug. High-Voltage (HV) side and Signal (S) sides are visually indistinguishable (except from a barely visible 'S' and 'HV' mark on the plastic). The central pin is used to crimp the wire; the other two pins connect into the hedgehog printed circuit boards and the threaded hole provides the connection to the gas manifold. The aluminium ring houses the O-ring used to realize the gas-seal; the same aluminium ring is also part of the ground contact since its outside will make contact (we hope) with the aluminium tube and the electronic components (capacitor and resistances) are soldered onto its inside. (b) A tube end with a crimped in end-plug and German locator. The German locator is invisible and, as opposed to the crimp on the end-plug, also the crimp on the locator is invisible! So you simply have to believe us.

of course it sits in the central region of the C-shape. A detailed view of this crimp is shown in Figure 8. The Indium on the copper tube improved the gas seal, in particular in the edge regions of the C-shape (as is evident from Figure 7). To further improve the gas seal we also covered the tip of the copper tubes with glue (Araldite 106). The optimal amount of Indium is fairly critical: too much Indium leads to frequent wire ruptures in the crimp region and too little Indium leads to leaky tubes. Even during the BOL and BML tube production we suffered occasional problems with the wire crimp. We consider the wire crimp an open issue; investigations are underway to try to improve the present scheme (quality of the copper tubes) or to adopt a more conventional wire crimp e.g. in addition to the copper tube. Let it be clearly understood that the copper tube was *not* selected in view of its wire crimp features, but in view of the possibility to feed the wire thru the end-plug automatically.

We also investigated the ground contact quality to some extent. A few short tube samples with an end-plug crimped at one end were cycled for a few days in an oven (from room temperature to 80°C and back). To enhance the humidity, and hence the corrosion, the inside of the oven was kept humid. We did not notice any degradation of the DC ground contact during this test. Similar tests were performed on tube samples with end-plugs, which in addition to the pressure crimp, were also connected to the aluminium tube wall via either point-welding techniques or ultrasonic welding techniques. As expected these additional ground contacts did also stay satisfactory after the cycling in the oven. The quality of the contacts after point-welding and ultra-sonic welding were also studied from microscope photos from successive layers thru the metal-metal inter-connection.

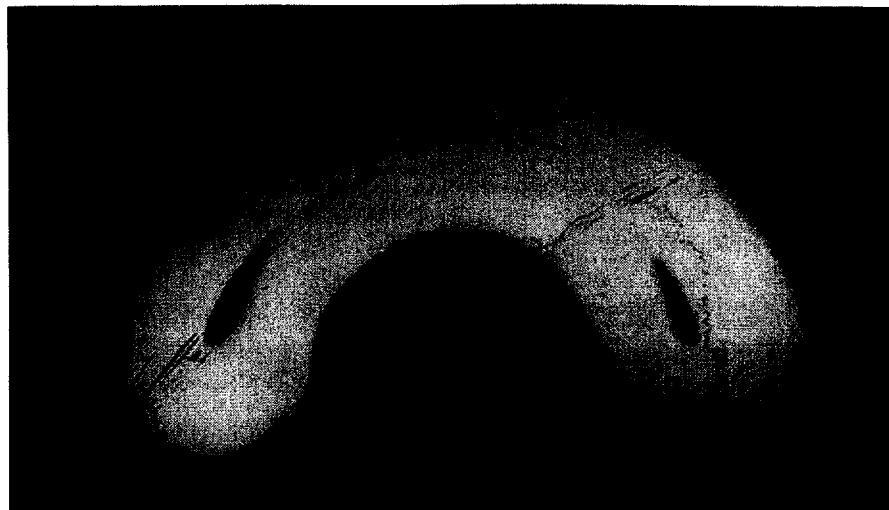


Figure 7: *Enlarged view (45×) of the copper tube used to crimp the W-Rh wire in place. The 50 μm diameter wire is clearly visible slightly out of the central region (on the left hand side). The large openings at the edges of the C-shaped crimp are not typical. During the production these openings were much smaller and in Frascati they improved further upon the crimp jaws and they find hardly any visible openings.*

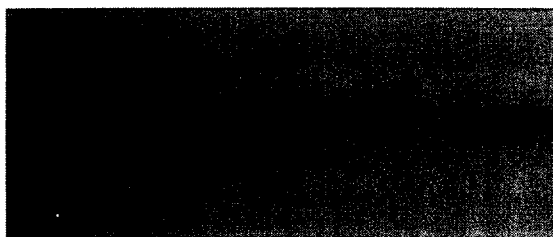


Figure 8: *Close up view of the wire crimped in the copper tube. The dark narrow band is the Indium, not air!*

Preliminary results indicate both methods really fuse the two separate aluminium layers (one from the tube and one from the aluminium ring on the end-plug) well together. These results should soon be available in a separate note (by G. Lion).

3 Tube Assembly

Early 1995 the CERN robot successfully wired two MDTs using 250 μm wall thickness tubes and dummy mechanical components (locators and end-plugs) made from Delrin. (Delrin has excellent sliding features w.r.t. aluminium.) This proved that the principle of automated as opposed to manual tube wiring was feasible. In a nutshell the successive steps were:

1. Mount one end-plug (left from the previous cycle, see point 5 below) and the three wire locators (two at tube ends and one at tube center) on two parallel rods at the correct locations, onto the wire which is already in place.

2. Slide the aluminium tube onto the end-plug and subsequently on the three wire locators.
3. Crimp the end-plug and the three wire locators in place within the aluminium tube. We started with a mechanical crimp, later we changed to an air-pressure crimp (shown in Figure 9). The details of the employed crimping scheme are *not* too relevant for the wiring scheme; more a matter of reliability, precision and, less so, cost.
4. Slide the aluminium tube, with the end-plug and three wire locators mounted within, back. During this step sufficient wire is rolled from the wire supply (for the subsequent tube) and the two parallel rods, originally positioning the end-plug and the three wire locators, retract from the tubes (of course it is really only the aluminium tube which moves; the two parallel rods stay basically in place).
5. Mount the final end-plug as well as the end-plug for the next tube to be wired. Crimp the final end-plug into the aluminium tube. Tension the wire to the required tension and crimp the wire in place. Also crimp the wire into the end-plug for the next tube. Cut the wire. This completes the fabrication of an MDT and leaves the setup ready for the next cycle i.e. the next tube to be produced!

In December 1995 we tried the same scenario for the production of the BOL tubes using real components: the Frascati end-plug (material: Noryl) and the German wire locators (material: Vectra) discussed before. This led to severe difficulties, partially due to imperfect alignment of the various components on the hypothetical tube axis and partially due to the large friction between aluminium and Vectra, the wire locator material. Also the clearance between tube inner diameter and component outer diameter could be improved upon³.

These difficulties led us to simplify the wiring scheme for the BOL tubes towards the in our view simplest manual (i.e. most likely to succeed) scenario:

1. Click the central wire locator around the wire and position this central locator rigidly between two long (about $\frac{1}{2}$ the length of a tube) large diameter (just below 30 mm) hollow rods. The W-Rh wire runs thru these rods and the central locator.
2. Slide the aluminium tube onto this central locator and crimp this locator in place within the aluminium tube. Remove one of the hollow rods.
3. Insert wire locator in tube end (around the W-Rh wire!) with an auxiliary device and crimp it in place, if it is a German locator; if it is an Italian locator, it is fixed in place by itself due to its tight dimension. Remove auxiliary device and do the same, using another auxiliary device for the end-plug (operation is shown in Figure 10). Crimp end-plug within the aluminium tube and also crimp the W-Rh wire within the end-plug (wire is *not* under tension at this moment).

³Of course this is only a long term option and it requires experimentation. Clearly the end-plug outer diameter can be substantially smaller than the tube inner diameter to optimise insertion of the end-plug. The gas seal is taken care of by an O-ring *after* deformation of the aluminium tube in the O-ring location. Similarly, the outer diameter of the locator can be optimised, *provided* we opt for locator fixation by either local or concentric deformation of the aluminium tube in the locator region as planned for the German locator. The Italian locator must remain slightly oversized since it locks in place by itself.

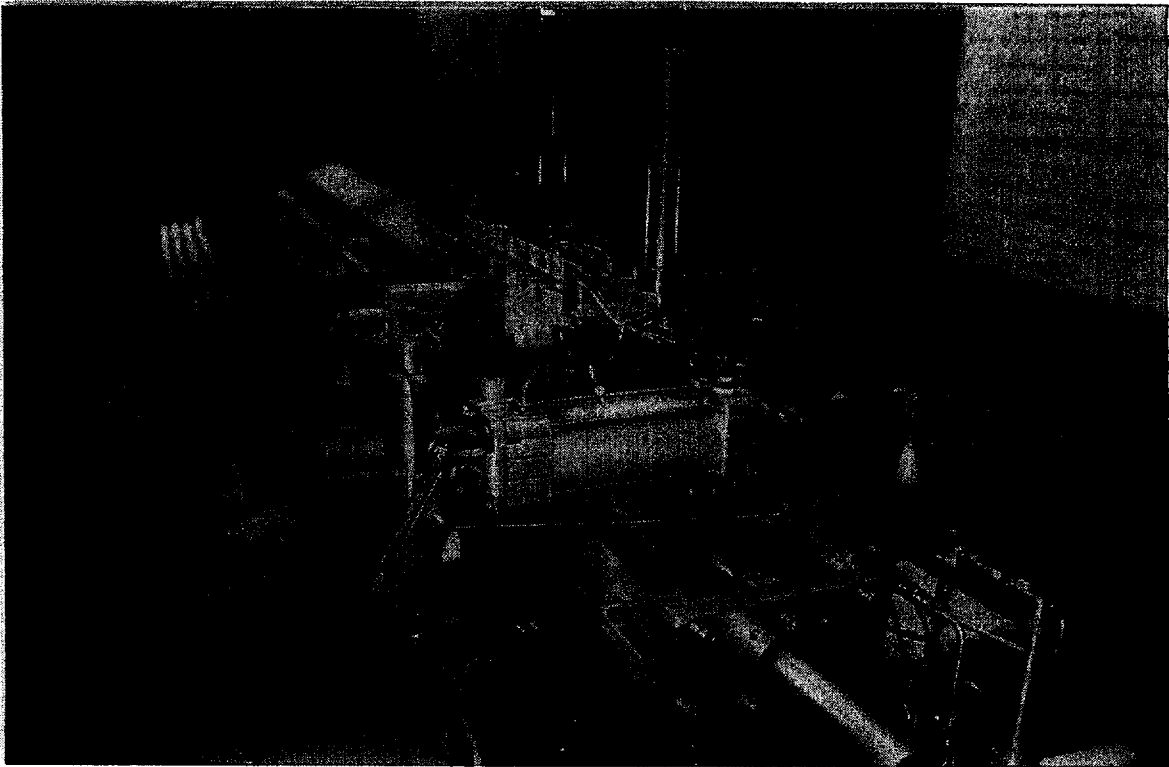


Figure 9: Overview of the end-plug crimp region of the wiring setup. The air-pressure crimpers as well as the mechanical crimpers used for the wire crimp are both visible (if you look hard). The air pressure crimper is basically a simple square brass block with an internal volume which can be brought to (high) pressure. The pressure is provided by a compressor which can deliver up to 330 Bars. CERN safety allowed us to go to maximally 200 Bars. The force is transferred from the compressed air onto the tube via a O-ring which gets pushed onto the tube. After some initial adjustments, notably on the guiding system visible in black, these air-pressure crimpers worked excellently.

4. Slide the aluminium tube, with the end-plug and two wire locators mounted within, back. During this step sufficient wire is rolled from the wire supply and the remaining hollow rod exits from the aluminium tube as well.
5. Mount the final wire locator as under step 3 and also mount the other end-plug as under step 3. This completes the fabrication of an MDT and leaves the setup ready for the next cycle i.e. the next tube to be produced!

The mounting gadget used for the insertion of an end-plug is shown in Figure 10. The gadget used for the mounting of the locators is similar. All gadgets are keyed to always mount the components in a well defined orientation w.r.t. the electronics pins on the end-plugs. With this scenario we wired all tubes for the BOL chamber. Typically 20-25 tubes were wired per day. In principle a few more tubes could be wired per day, but in parallel we had to modify and/or test some of the components (notably the end-plugs) as well. Apart from occasional wire ruptures (at the 2% level; *not* always in the wire crimp region but also often at a random location) and problems with the gas seal (improving from as poor as 5% at the start to about 1-2% at the end), no real difficulties were encountered. This, among others, convinced us that the sliding of a tube over a correctly positioned and rigidly held wire locator is possible. With this in mind we went back to a more automatic

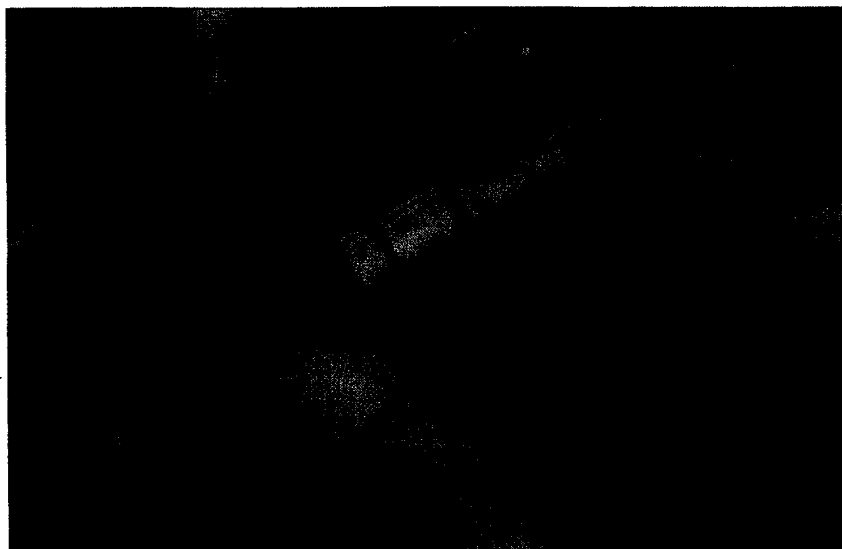


Figure 10: *Close-up view of the gadget used to insert the end-plugs into an aluminium tube. The gadget engages onto the pins which later-on connect into the hedgehog electronics boards. The gadget positions these pins w.r.t. the inner tube surface. The orientation is fixed using the groove visible in the gadget near the very top of the photo.*

wiring scheme for the production of the BML tubes.

With the BOL experience in mind we modified the positioning of the wire locators as well as the positioning of the end-plug on the two parallel rods. In the original scheme the components were only held near their center over a small region. This allowed for vibrations of the components and also made it hard to align them properly. We modified the fixation of the wire locators on the two parallel rods as indicated in Figure 11. The same figure also shows the end-plug mounted on the same rods. The four plastic flaps are spring loaded; this allows them to collapse into slits machined inside the rods to make it possible to retract the aluminium tube and together with it the locators mounted in the tube, leaving the rods in place. Similarly we changed the fixation of the end-plug on the rods into a more rigid mount. We added a guiding piece in front to minimise friction between the aluminium of the tube and the aluminium of the end-plug. With these modifications we wired all of the long (4005 mm long) BML tubes (that is 285 tubes) along the first listed scheme above. We did not push for full automatism since we first wanted to make sure the principle performed according to expectations. In Table 2 we indicate what was left to the automate and what was done by hand. All in all this scheme worked satisfactory, we routinely produced 40 tubes a day; where we again prepared components in parallel. The minimal time required for a single tube was about 5 minutes (this also implies a higher per day rate would be feasible, already with the present setup). Also this way the tubes could be wired by a single person.

In the future we intend to revive the automatic threading of the wire thru the end-plugs as well as the automatic loading of the last end-plug. We might also investigate the automatic loading of the three locators and the first end-plug as originally foreseen. In parallel we will investigate the important issue of the wire crimp⁴. Finally we eventually

⁴To date the wire crimp used for the BOL and BML tubes is different from and poorly tested compared to those used for the other MDT prototype chambers. Either our scheme must be certified to be performant and reliable, or we have to include one of the standard and well tested methods developed by

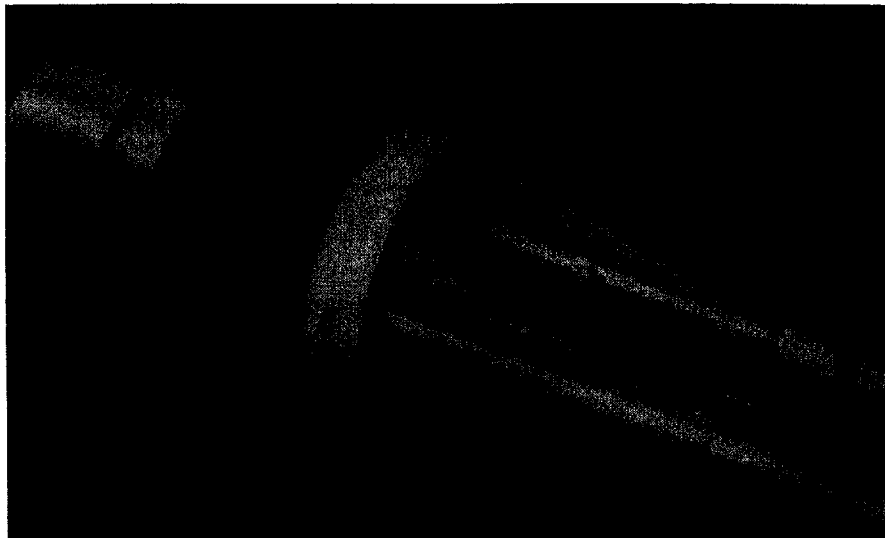


Figure 11: *Close-up view of the mount of a wire locator and an end-plug on the two parallel rods used to position the three wire locators and one end-plug before the aluminium tube is glided onto them. The white triangular plastic pieces (fins) pushing against the wire locator are spring loaded and can be retracted to allow for the removal of the rods from the aluminium tube.*

intend to re-evaluate the possibility of a mechanical crimp for both the wire locators and the end-plugs. This time *not* using a rolling device but using a mechanical chuck similar to those on any conventional drilling machine. We do feel that such an effort is justified in view of the many man-years we might spend on the production of the 300.000 MDTs required for the ATLAS muon spectrometer.

4 Tube Quality Control

The critical aspects of an MDT are: a very low leak rate ($< 10^{-8}$ [Bar \times Litre/Second]), a precise wire location with respect to the outer tube wall ($< 20 \mu\text{m}$ in both transverse coordinates). In addition we aim for a precision on the wire tension of about 1 – 2%. Finally the MDT should of course operate as a particle detector i.e. it should exhibit a moderate (nA level) leak current at the operation high voltage of about 3.2 kV (with the correct(!) gas mixture). In the following sections we describe how we verified these tube quality parameters. Wherever applicable we also indicate our preferred quality control setup and we also indicate shortcomings of our setup.

4.1 Leak rate measurements

Our original, simple, leak rate measurement setup was designed when the leak rate specification was still $< 10^{-6}$ [Bar \times Litre/Second]. The setup, shown in Figure 12, allowed to connect up to 40 tubes in parallel to a 200 Bar gas bottle (Argon). All tubes are pressurised and subsequently the input valve on each tube is closed. The initial pressure,

others. It goes without saying that our scheme is ‘easy’ to automate and that the other schemes are per-formant!

Step	Automated	Manual	Time [sec]
1		<i>previous cycle: position end-plug, crimp wire</i> position the two German locators	
2	tube movements		
3	crimps	switch flipping to initiate crimps (wire -, end-plug - and locator crimps alike)	
4	tube movements wire feeding		
5	locator crimp end-plug crimp wire crimp	mount the Italian locator switch flip to initiate crimp mount (and feed wire thru!) last end-plug switch flip to initiate crimp apply wire tension switch flip to initiate wire crimp	

Table 2: *Sketchy indication of how much went automatic and how much went by hand during the production of the 285 long tubes for the BML prototype. Note: all three wire locators could have been positioned under point 1, if we would have used German locators only. Due to the lack of German locators we had to use at least one Italian locator for each BML tube. The Italian locator we mounted near the end of the cycle (point 5).*

$P_0 \approx 4000$ mbar, and temperature, $T_0 \approx 300$ K, are (automatically) recorded⁵. Typically after about 15 hours, the pressure, P , in each tube is measured by opening the valve of that particular tube. Also the temperature, T is recorded. Finally the leak rate, \mathcal{L} , is calculated as follows:

$$\mathcal{L} = \frac{(P_0 - PT_0/T) \times V}{\Delta t} \quad [\text{Bar} \times \text{Litre/Second}]$$

In this expression, Δt is the time the tube was left under pressure and V is the volume of the tube (4.0 litres for long, 5700 mm, BOL tubes and 2.8 litres for long, 4005 mm, BML tubes). If the accuracy of this leak rate determination is limited by the pressure measurement precision of about 5 mbar, the expected precision (r.m.s. of the measured distribution of leak rates) would be:

$$\begin{aligned} \text{BOL: } \Delta\mathcal{L} &\approx \frac{\sqrt{2} \times 0.005 \times 4.0}{15 \times 60 \times 60} \approx 5.4 \times 10^{-7} \quad [\text{Bar} \times \text{Litre/Second}] \\ \text{BML: } \Delta\mathcal{L} &\approx \frac{\sqrt{2} \times 0.005 \times 2.8}{15 \times 60 \times 60} \approx 3.6 \times 10^{-7} \quad [\text{Bar} \times \text{Litre/Second}] \end{aligned}$$

As is evident from results shown below, this estimate is too large. This is easy to understand: our tubes typically are significantly better than the precision of this setup. This means the pressure stays unchanged and we only have to deal with the uncertainty due to the temperature measurement (since we are *not* working in a clean temperature controlled environment). The temperature measurement precision was about 0.1 °C. This corresponds to about 1.3 mbar pressure uncertainty. With this estimate, the measurement

⁵We really recorded the over-pressure only. I.e. we did neglect atmospheric fluctuations! This is an oversight and should be corrected in the future.

precision becomes:

$$\begin{aligned} \text{BOL: } \Delta\mathcal{L} &\approx \frac{\sqrt{2} \times 0.0013 \times 4.0}{15 \times 60 \times 60} \approx 1.4 \times 10^{-7} \quad [\text{Bar} \times \text{Litre/Second}] \\ \text{BML: } \Delta\mathcal{L} &\approx \frac{\sqrt{2} \times 0.0013 \times 2.8}{15 \times 60 \times 60} \approx 0.9 \times 10^{-7} \quad [\text{Bar} \times \text{Litre/Second}] \end{aligned}$$

This is in good agreement with the results found for the r.m.s. on the BOL tubes!

All tubes with a noticeable leak were at first rejected; i.e. only tubes with a leak below our measurement precision were kept. Note that we performed this test at $P \approx 4000$ mbar, so we are slightly over-estimating the leak rates for the real muon spectrometer.

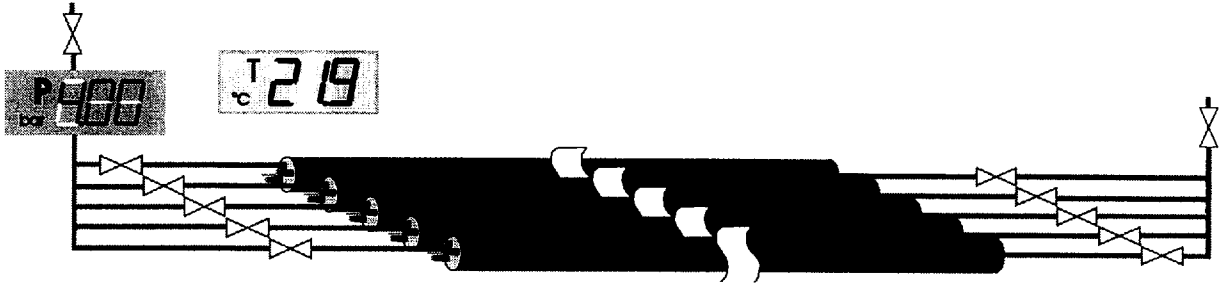


Figure 12: The simple leak rate measurement setup. Up to 40 tubes could be tested simultaneously.

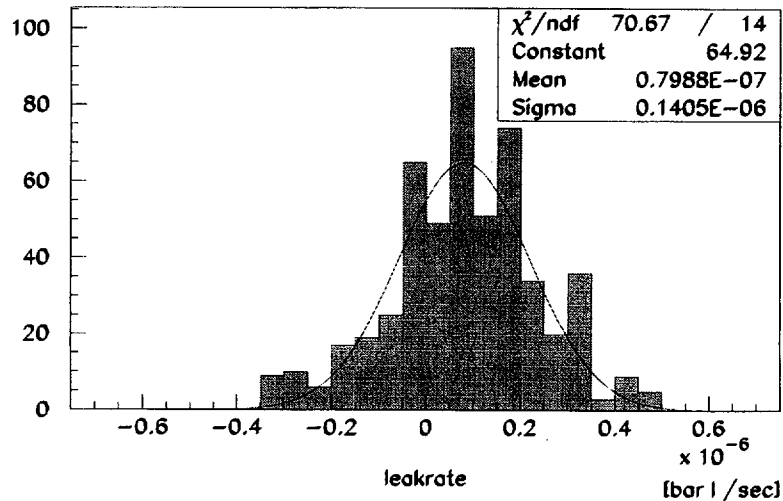


Figure 13: Measured leak rates for all tubes.

The results of the measurements on the BOL tubes are shown in Figure 13. As expected for good tubes the distribution is consistent with no leak found at all. The r.m.s. of the distribution, 1.4×10^{-7} [Bar \times Litre/Second], is in excellent agreement with the expectation from the temperature measurement precision alone. Whenever a tube was found leaky we inspected the cause of the leak using a simplistic setup: we slide a transparent holder around the tube end, fill this holder with water, pressurise the tube and we look at the air bubbles to establish the origin of the leak. The holder is shown in Figure 14.

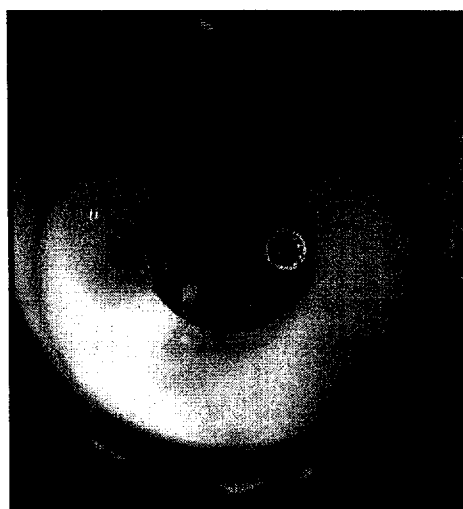


Figure 14: *Holder used to find leak location in end-plug region. Rather poor figure; it shows the plastic holder as well as a tube mounted within. The crew on the end-plug serves to close this end of the gas connection. The other end of the tube is put at $P = 4$ Bars and if the tube would be leaky one would immediately see a bubble trace.*

Three different leak causes were found, in decreasing order of importance:

1. Within the potting in the end-plug. This was the most common leak cause; typically at the 1-2% level by the end of the BOL production. This even with end-plugs already tested for leak tightness *prior* to tube production. It indicates that from time to time the potting can not deal with the pressure exerted by the 190 Bar crimp on the end-plug. We found one tube where the potting had a large crack (and hence an enormous leak). During the BOL tube production several improvements were made to the end-plug assembly. This improved the leak behaviour of the end-plugs, but it still needs to be improved further or we must avoid to rely partially on glue (the potting) for the gas seal. Improvements were: improved mixing of the two component glue, gluing in a correct temperature environment, de-greasing of notably the aluminium ring, the addition of more glue. Possible future improvements are roughening of the surfaces to be glued together and better glue access to the critical region between aluminium ring and the plastic. The latter implies changing the molds used for the casting of the plastic pieces.
2. Within the copper tube used for the wire crimp. These leaks were only found initially when we did not cover the tip of the copper tubes with Araldite 106. These leaks also correlated well with the amount of Indium used. For the later part of the BOL tube production and for the entire BML tube production we did not find leaky wire crimps.
3. Between aluminium tube and end-plug. This means the end-plug crimp failed or the O-ring in the end-plug region malfunctioned. During the BOL production only few of these leaks were found. For the BML production we found many (5%) tubes leaking in this region. This only on the HV side. This is because for the BML production, the aluminium tubes must slide along the HV end-plug. From time to time the O-ring got displaced and/or the HV end-plug tilted a bit. Of course this will deteriorate the gas seal quality. A likely solution of this problem is to slightly

modify the groove used to hold the O-ring in place: e.g. from the two-step groove (barely visible in Figures 6 and 11) to a one-step groove. It should be noted also that the O-ring location jumped around in the period preceding the BOL production. We finally opted for the presently used location, on the aluminium ring, in view of the reliability of the air-pressure crimp. Originally the O-ring was supposed to sit on the plastic at the end of the aluminium ring. This is to be preferred because it makes the gas seal far less dependent on the potting used to insulate the HV in the end-plug from ground. (Possible disadvantage: an O-ring seal between plastic and aluminium might be less reliable than an O-ring seal between two aluminium surfaces.)

4. Faulty tubes. This problem we only experienced with the BML tubes. We found 1 tube with a small (but very leaky), barely visible, pin-hole in the tube wall. For one other BML tubes we could not find a leak in the end-plug regions, despite the fact that the tube was found leaky in our test.

Integrated over the complete BOL and BML production we found about 7% of the tubes leaky after these tests. All of these tubes were re-glued, i.e. more glue was added onto (both) end-plug ends and the tubes were tested again. This way we recuperated all, except 2, of the BOL tubes. For the BML also a couple of tubes remained leaky.

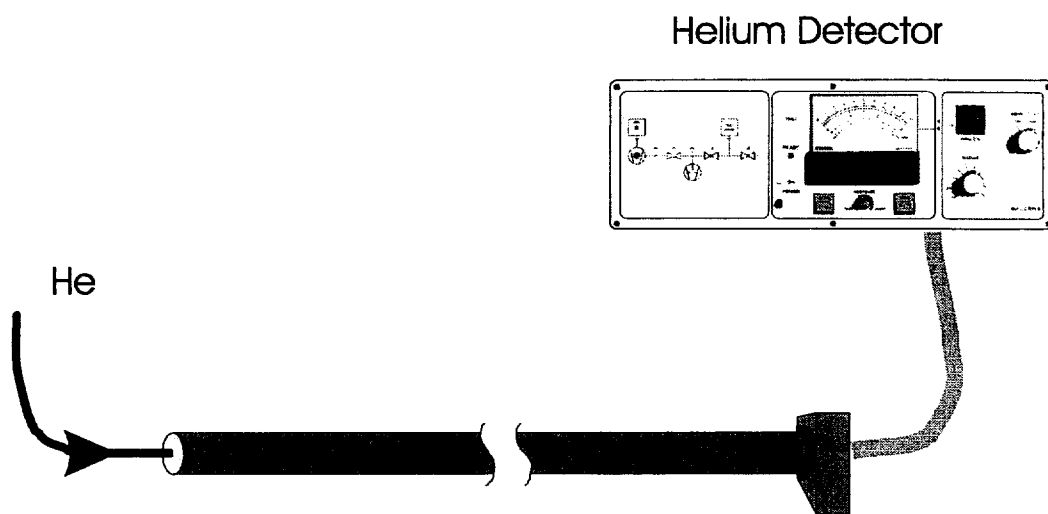


Figure 15: *Leak rate measurement setup using a helium leak detector.*

As we all know the specification on the leak rate of an MDT changed significantly due to the 'back diffusion' issue. Today we work under the assumption that an MDT should meet a very tight specification of the leak rate of:

$$< 10^{-8} \text{ [Bar} \times \text{Litre/Second]}$$

Of course this number is completely out of reach with our simple leak rate measurement setup (unless you want to wait 10-20 days for every batch of 40 tubes). So we prepared a setup around a helium leak rate tester (Balzers, HTL 100). This to inspect the real leak rate on a sub-sample of our tubes. This setup is shown in Figure 15. It is straightforward: we simply pressurise a tube to 3 Bars using helium (really an air:helium mixture in the

ratio 1:2, but that is irrelevant and can even be corrected for). We connect the vacuum pump of the helium leak detector to the end region of the tube and measure the rate at which helium escapes from the tube end (i.e. end-plug region). This is *exactly* what will be the leak behaviour in the real spectrometer in the future. The only difference is that we measure it using helium instead of argon. That simply means we are again finding a pessimistic answer (and one could even correct for it to some extent). The upshot of these measurements, based on a low statistics sample of about 20 tubes, is that we found that our typical tube is leaking at a few times 10^{-9} [Bar \times Litre/Second] i.e. just below the above quoted specifications (realize: each tube has *two* end-plug regions!). The draw-back of this method is that it is cumbersome (connection to the vacuum pump) and that it took a while because we inject the helium into one end and measure the emerging helium at the other end (verify this, velocity of He₂ molecules are of order 10^3 m/s at $T \approx 20^\circ\text{C}$!). This remains to be investigated in more detail, but clearly a better setup would evacuate the tube *before* one injects the helium. It also would be better (both in view of money *and* in view of the measurement) to recirculate the helium after a tube has been tested, instead of simply venting it into the environment.

4.2 Wire tension measurement

The wire tension is important because it enters into the prediction of the wire location in the regions in between the wire locators. Both the BML and the BOL tubes have central wire locators so the free hanging region is reduced by a factor two; the maximum of 2810 mm is of course attained by the long BOL tubes. The aim on the wire tension precision is about 1-2%. We realised the wire tension by stretching the wire with a simple weight just before we make the last wire crimp. For BOL we used a weight of 250 grams and for BML we used a weight of 300 grams. For the BOL tubes we also ‘kind-of’ pre-tensioned the wires briefly at a tension of 400 grams. (This not really in view of the reduction of wire tension changes in time (‘creep’), but more to avoid wire rupture in a partly finished tube). We measured the wire tension in a completed MDT with a wire stretch meter, originally designed by the Frascati group and nowadays marketed by CAEN (Mod SY 502). Our unit had to be slightly modified to measure the tension for the long BOL tubes (200 cm is the standard limit on the wire length). The setup is simple and requires in addition to the CAEN unit only two cables and a magnet. The input parameters to the measurement are: the W-Rh wire diameter (d), the wire length between supports (L) and the density of the wire material (ρ). The wire stretch meter determines the oscillation period (T) of the first mode which is, using the input parameters, converted to a wire tension (F):

$$F = \frac{d^2 \rho L^2}{T^2 g}$$

In here $g \approx 9.81 \text{ m/s}^2$ is the acceleration in the earth’s gravitational field. You pick the appropriate units!

The setup is shown in Figure 16. The measurement precision is more than adequate (better than 1%). We suffered more from temperature differences (and fluctuations) between the time of tube production and the time of tube inspection. This is evident from Figure 17 in which we show in the second plot the tension versus the temperature difference between the time of tube production and the time of tension measurement.

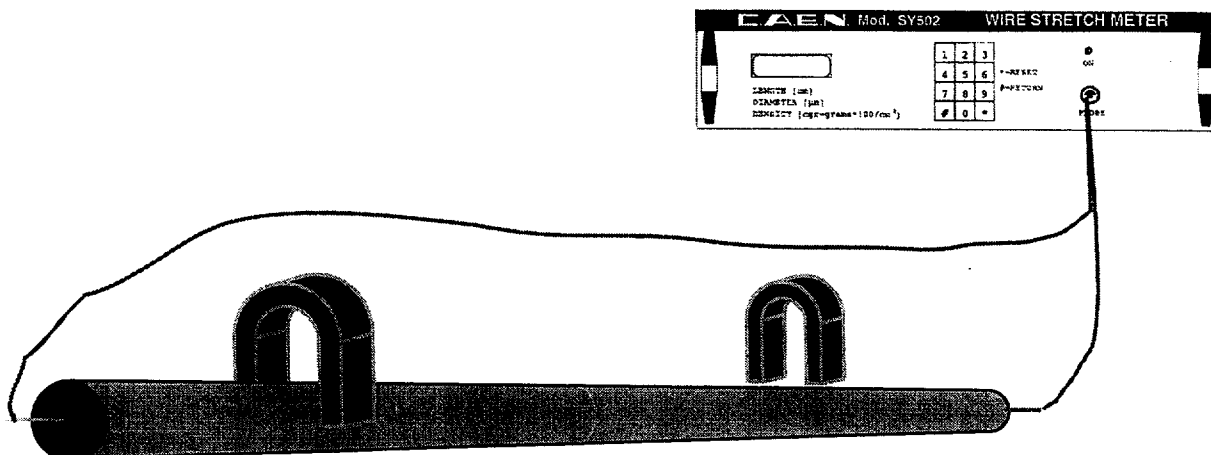


Figure 16: *Wire tension measurement setup.*

There is an obvious correlation due to the different thermal expansion coefficients of aluminium ($24 \times 10^{-6} / ^\circ C$) and tungsten ($4.4 \times 10^{-6} / ^\circ C$). The fitted slope of $1.3 \text{ gram}/^\circ C$ is in rather poor agreement with the expected slope of about $0.7 \text{ gram}/^\circ C$. In the first figure we show the measured wire tension after we corrected for the temperature effect. The r.m.s. of 4.3 grams is just below the 2% level. However, it must be noted that the r.m.s. on the wire tension of the tubes in the BOL chamber will be larger since for the BOL prototype the temperature correction can not really be performed: the chamber will be operated at a certain temperature whereas the tubes have been produced at various different temperatures. (In principle we could of course take this into account since we know for almost all tubes the tension at the wiring temperature.) Another contribution to the *measured* wire tension fluctuation is the W-Rh wire diameter. For the BML we noticed an apparent change in the wire tension of 2% after we changed to a new spool. This was attributed to a 1% change (i.e. $0.5 \mu\text{m}$) in the W-Rh wire diameter (see above and note: the *real* wire tension did *not* jump, only our measurement changed since we gave the wrong wire diameter value as input).

In Figure 17 is also shown that some BOL tubes have a wire tension far away from the central value i.e. the uniform distribution between 200 and 300 grams. We do *not* have an unambiguous explanation for this effect. For the early BOL we manually held the wire in the correct orientation (this to have the wire located in the central part of the C-shaped copper tube shown in Figure 7). It was noticed that this led to a larger scatter on the wire tensions. For the later produced BOL tubes and for all BML tubes, we mechanically located the wires in the correct azimuthal orientation. For the BML tubes we did *not* observe these large deviations from the nominal (300 gram for BML tubes) wire tension.

4.3 Wire location measurement

A precisely, $< 20 \mu\text{m}$ in the transverse plane, located central wire w.r.t. the tube outer wall is a distinctive feature of the MDT. Within ATLAS two scenario's have been developed to verify the wire location:

1. X-raying of a single tube (originally proposed by colleagues from Brandeis),

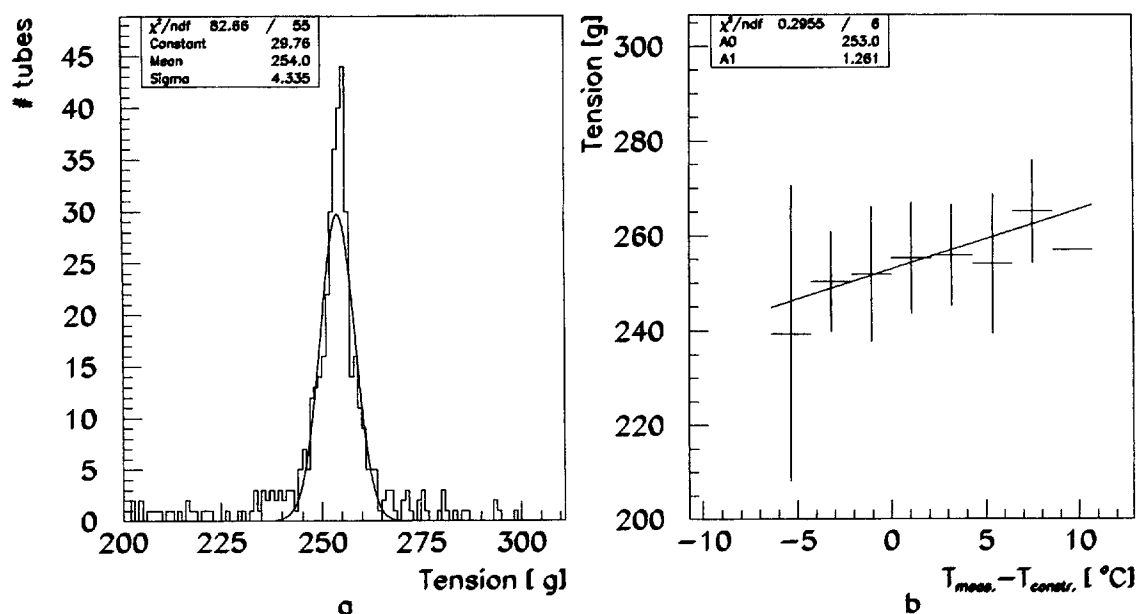


Figure 17: Wire tension for BOL tubes. (a) Tension, after correction for the temperature difference (b) Tension versus the temperature difference.

2. X-raying of a complete MDT chamber (originally proposed by colleagues from Dubna).

For individual tubes we of course only used the method proposed by Brandeis. Here we only want to summarise the essentials and we want to present our findings on and experience with the BOL and BML tubes. For reference we include an earlier note, detailing the method and some preliminary studies, in appendix C.

4.3.1 Method

The principle of the wire location measurement is simple: the MDT is located into a jig, ideally equal to the basic unit of the jigs used for subsequent stacking of tubes into a real MDT chamber. In our case the jig was very similar to the NIKHEF jiggling, including a vacuum suction head to suck the tube into the jig. Around the jig several, four in each of the two views, reference wires are rigidly mounted. Two (stereo) pictures are required to determine the wire location w.r.t. the reference wires, i.e. the jig, in the transverse plane. That can either be achieved with a single X-ray gun which can swing around; we opted, instead, for a stereo setup using two (dental, Gendex, Gx-770) X-ray guns. In our setup the X-ray images are registered on commercial (dental) X-ray film. These films are developed and subsequently scanned under a microscope to determine the relative locations of the four reference wires and the wire inside the tube. From this information the location of the wire w.r.t. to the jig can be calculated. In our case we were not so much interested in the absolute location, but more in the scatter in the wire locations

from tube to tube i.e. the r.m.s. of the distributions⁶. The jig is shown schematically in

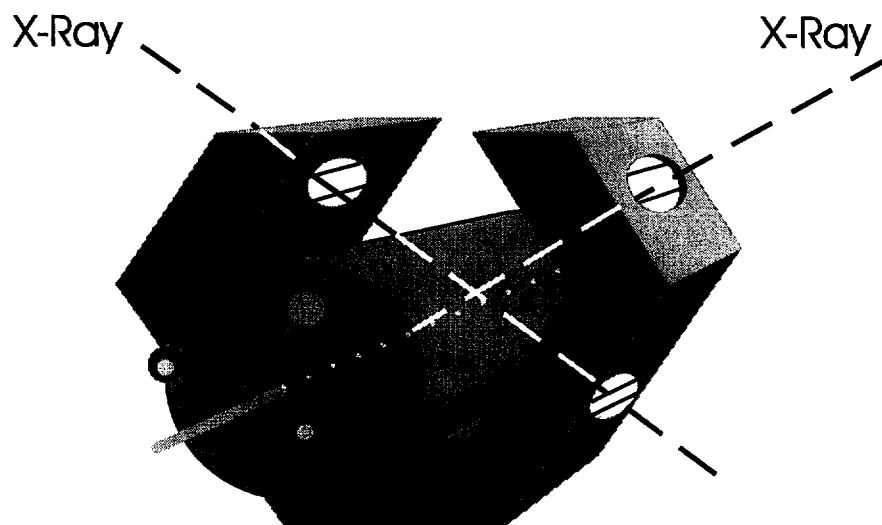


Figure 18: *Wire location measurement setup. Three of the four windows housing two, horizontal, reference wires each are clearly shown. Also the two X-ray beams are indicated. The X-ray films are not shown, they would sit in the lower left and lower right corners of the jig; snug to the lower window with the reference wires.*

Figure 18. For each tube we inspected the wire location in the critical regions: on the relevant side of the locators at the tube ends (positions *a* and *d*, see the appendix C) and on both sides of the locator in the tube center (positions *b* and *c*, see appendix C). To limit the amount of dental film these 4 locations are recorded on a single X-ray film (i.e. two films per tube: one for each of the two cameras). A typical example is shown in Figure 19.

4.3.2 Error sources and defects

Apart from the *real* wire mis-placements we want to assess, many effects can contribute to *apparent* wire mis-placements:

1. The mounting of the tube in the jig. I.e. the tube must be in firm contact with the faces of the jig.
2. Deformations of the tube outer wall from an ideal circle. (See appendix C for this).
3. Mis- or poor alignment of the X-ray films in the jig. (See appendix C for this).
4. Bad or poor sanning of the X-ray film. (See below and also appendix C for this).
5. Bugs in the analysis program used to convert the scanning results into wire locations in the *XY* plane. (See appendix C for this).

⁶The X-ray method also allows the determination of the absolute location of the wire w.r.t. the jig. This requires a separate analysis of a set of stereo images of a single tube (or simple cylinder) positioned at various (12 in our case) azimuthal angles in the jig. This is explained in detail in the appended note. For the BOL tubes we did take calibration data; however because of lack of time (and because we claim it is not too interesting) we did not pursue the analysis hereof.

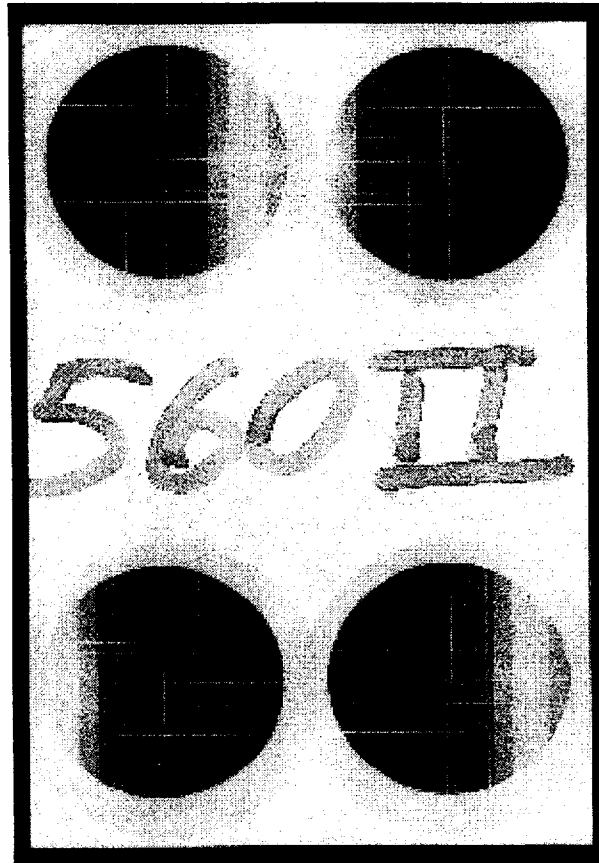


Figure 19: X-ray film example. Each sub-picture corresponds to one location along the tube. The five (four fiducials and one for the real wire in the tube) horizontal wire traces are the important ones. The three vertical traces on this film allow the separation of the two films forming a stereo pair (the other one has only two vertical traces). The vertical traces also could (but did not really) facilitate the alignment of the X-ray guns and jig. The bright vertical bands are the shadows of the locators, German ones for this film. For the Italian locators a clear gap would have been visible in between the two half-locators.

Our earlier study (see appendix C) showed all of these effects, except the first one, to be ir-relevant on the $\leq 20 \mu\text{m}$ level of precision we are aiming for. (Note: point 2, deformations from an ideal circle of the tube outer wall, are serious. However, as long as all wire locators are mounted in the same azimuthal orientation, we can correct for this effect.) As an illustration we show the X-ray film scanning precision (the most time consuming affair) achieved for the BOL tubes. Each X-ray film was measured twice; two fiducial wires sit very near the X-ray film, two sit about 80 mm away and the MDT wire sits halfway. The X-ray guns sit about 800 mm away. This implies that not all shadows are equally sharp and we expect differences in the scanning precision accordingly. This is nicely illustrated in Figure 20. As expected the far fiducial wires are measured worst ($5.2 \mu\text{m}$) next the MDT wire ($3.9 \mu\text{m}$) and finally the near fiducial wires ($3.3 \mu\text{m}$). Because we measure twice, the real precision input to the analysis program is a factor $\sqrt{2}$ better.

The precision of the mounting of long MDTs into the jig is a concern. Of course, the risk of bad mounts of a real 5700 mm long tube into the jig is of course very different compared to the risk of bad mounts of the dummy 200 mm long tube used for our earlier

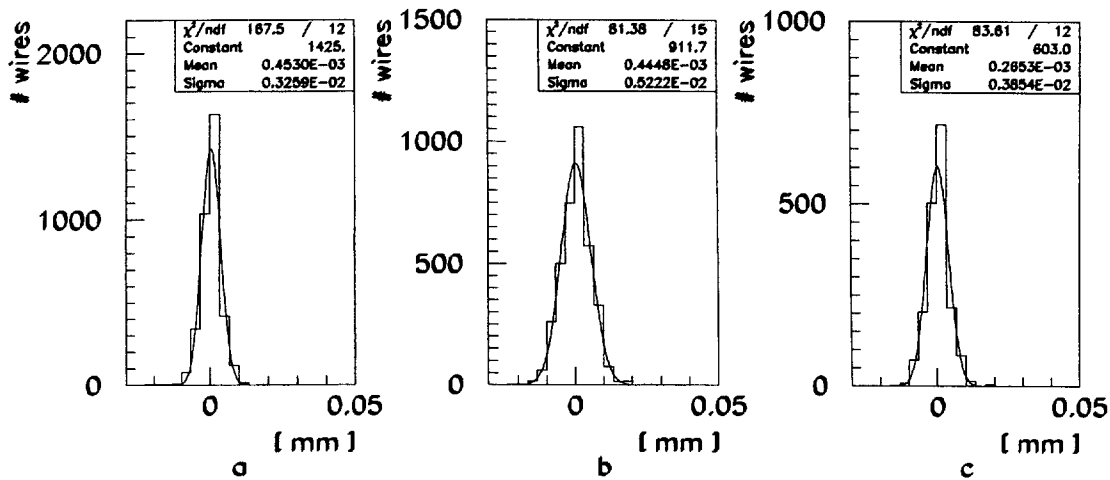


Figure 20: Precision of the scanning of the X-ray film: (a) near reference wires (b) far reference wires (c) MDT wire.

investigations presented in appendix C. The short dummy tubes were *only* held by the vacuum suction nipple mounted in the jig. This lead us to pay most attention to the measurements of the central wire locator. Measurements near the dummy ends suffered from a poorly balanced tube. For the long MDTs we added two long aluminium V-grooves, one on either side of the X-ray jig, to provide additional support for the tube. However these V-grooves and the X-ray jig were not well aligned. This is not so serious for the measurements on the wire locators at the tube ends since for these the tube is only constrained by the V-groove on one end, and the aluminium tubes are fairly flexible. For the measurements on the central locator, however, the tube is constrained on either side by the poorly adjusted V grooves. Half-way during the production of the BOL tubes it became clear that it was difficult to get the tube mounted correctly into the X-ray jig for the measurements on the central locator. This particular in the horizontal plane of our setup which corresponds to the X axis indicated in the figures of the wire locators (Figures 4 and 5). Apart from the poor alignment, the poor mount was also due to the vacuum suction nipple which deteriorated significantly due to tubes sliding on top of this nipple (about 1000 tubes were measured!).

4.3.3 Results

Both BOL and BML tubes have been produced with different combinations of German and Italian locators. The statistics are listed in Table 3. At the centre location we only used German locators. For the BOL tubes the Italian locators were inserted manually from the near tube edge. For the 'I-D-I' BML tubes, one of the Italian locators was moved thru the complete tube i.e. as for the German locators. Note that the Italian locator is not well adapted for this motion since it separates in the transverse plane. Therefore, for all 'I-D-D' tubes, the Italian locators were always inserted manually from the near tube edge.

Chamber	D-D-D	I-D-I	I-D-D	Total
BOL, 5700 mm	288	277	0	565
BOL, 5180 mm	0	45	0	45
BML, 4005 mm	0	117	158	275
BML, 3460 mm	0	55	0	55

Table 3: *Distribution of locators in the produced BOL and BML tubes. ‘D-D-D’ means three German locators, ‘I-D-I’ means Italian locators at the tube ends and a German locator at tube centre, etcetera. The reason for the different combinations are twofold: (1) lack of German locators (expensive, about 3.9 SFr/piece!) and (2) the wish to evaluate the Italian locators (cheap, less than 1.0 SFr/piece!) as well.*

BOL tubes

For the BOL tubes, the results on the wire locations are summarised in Figures 22, 23 and 24.

BML tubes

For the BML tubes, the results on the wire locations are summarised in Figures 25 and 26. Several remarks can be made concerning these figures:

- The results on the central locator, positions b and d , (always German for these tubes) are significantly worse compared to those on the edge locators, positions a and c . We claim this is due to the poor inter-alignment of the V -grooves and the X-ray jig as mentioned before. This was clear from the X-raying of the tubes: before every exposure we always tapped the tube to verify its position in the jig. At the central locator position the tube was clearly *not* snug into the V -block. Therefore the results on the central locator reflect more the positioning of the tube than the quality of the central wire locator.
- Generally the results in the X (horizontal) direction are better compared to those in the Y (vertical) direction. This is also *not* related to the wire locators but is again due to the positioning of the tubes in the V -block. This we verified by scanning 10 tubes in the usual orientation *and* in a 90° rotated orientation (i.e. interchanging X and Y). Preliminary results hereof indicate that X and Y localising power of the wire locators are similar. I.e. in the rotated pictures, the Y coordinate comes out better compared to the X coordinate!
- In many distributions double peaks are visible. This is e.g. very clear in Figure 25 for the tubes with numbers from about 200 onwards. This systematic effect is almost certainly due to the twofold ambiguity⁷ in the mounting of the wire locators (German and Italian alike). For the German locator we noticed, and solved, this already during the BOL production. For the Italian locator we, by mistake, did not eliminate this ambiguity. For the BML, we explicitly investigated the systematics by producing tubes numbered 194-229 with both edge locators mounted one way

⁷Despite the symmetric halves, the German locators can be mounted in two different ways into a tube and the Italian locators can be mounted in four different ways into a tube. If the locators would be perfect, i.e. centre square exactly in the centre of the locator, all two (or four) ways would yield the same wire location. However, locators are im-perfect. This leaves two ambiguities (the four ambiguities for the Italian locators are pairwise indistinguishable because of the two symmetric halves).

and tubes numbered 230-355 with both edge locators mounted the other way. The results, in particular in the X direction (Figure 25a and d), are striking: at the change-over, tube numbers 229/230, the X coordinate jumps by about $50 \mu\text{m}$. This confirms that the double peaks are due to this ambiguity. It also implies that the real localising power of, at least the Italian, wire locators is given by the excellent r.m.s. of a narrow peak! We are still investigating the rather large size of the jump: a priori we expected the effect to be at most half of the dimension of the central square hole in the wire locators i.e. at most $30 \mu\text{m}$. (The effect is far less pronounced in Y . This is either due to the aforementioned worse performance in the Y direction or it is due to the fact that the two ambiguities differ less in the Y coordinate than in the X coordinate.)

4.3.4 Work still in progress

1. Conclude on the two-fold ambiguity in the mounting of the locators.
2. Evaluate in more detail the tubes which have been measured at a 90° rotated angle. Is the localising power of the locators the same in X and Y directions?
3. Conclude on the differences between the German and the Italian wire locators.
4. Study a few tubes in great detail i.e. mount tube in various azimuthal locations and make X-ray pictures.
5. Study wire vibration amplitude from X-ray picture(s) of a tube in operation.
6. Investigate long tubes without a central wire locator (produced some already, to be included in the BOL prototype, 380 gram wire tension).

Before these investigations are finished we can not really determine the precision on the wire locations. However, given that we on several occasions observed r.m.s. values on wire locations of samples of more than 100 tubes which are in the $10 - 20 \mu\text{m}$ range (e.g. Figure 24a, b, d and Figure 25a, b, c, d), we do feel confident that our wires are positioned to better than $20 \mu\text{m}$. I.e. we assume that the double peaks visible from time to time in e.g. Figures 22 - 26 are due to wire locator mounting ambiguities. We also assume that the poor results at the central wire locator are due to the setup, similarly for the poorer results in the Y direction.

4.4 Tube operation

In principle a leak tight tube with a correctly tensioned and precisely located central wire should work. Early on, we still decided to also run all of our BOL tubes thru a source and/or cosmic test. This turned out to be very cumbersome, partially due to the effort it took to get a good gas mixture (Ar : N₂ : CH₄ 91:4:5 mixture) into the tube and due to the humidity in B168 (surface currents on the outside of the end-plugs). As a result, we quickly gave up on the cosmic test. Only with the first tubes produced we looked successfully for cosmics. We even had one tube which nicely registered cosmics at 22 Hz, consistent with the 18 Hz expected. (A 5700 mm long BOL tube should see about

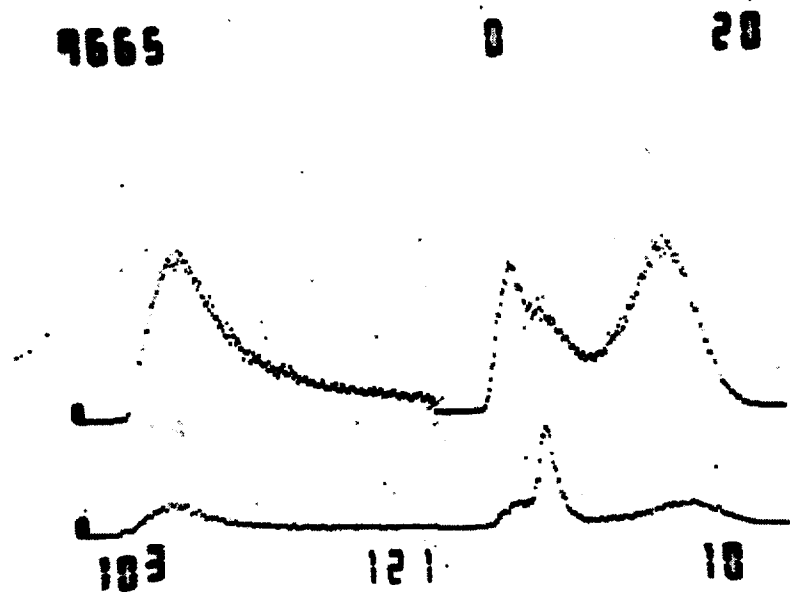


Figure 21: Spectra of ^{90}Sr (top left corner) and ^{241}Am . The latter is shown with (bottom right corner) and without (top right corner) a Molybdenum foil to select mono-chromatic γ rays. The bottom left corner shows a noise spectrum obtained at a 100 times longer exposure time than the signal spectra.

$30 \times 5700 \text{ mm}^2 \times 10^{-4} \text{ Hz/mm}^2 \approx 18 \text{ Hz}$.) Instead we inspected all tubes for response to a ^{90}Sr source and occasionally for the response to an ^{241}Am source. For this we operated the tube at 3300 V. At this voltage the leak currents ran from as low as a few nA to as high as $1 \mu\text{A}$. The latter we attributed (perhaps heuristically) to the humidity. Typical ^{90}Sr and ^{241}Am spectra (with and without a Molybdenum foil) are shown in Figure 21. From these tests we concluded that the BOL tubes indeed perform as a gaseous particle detector. We also found five tubes which failed this test. Three of the five had a broken wire (also already visible in the wire location measurement and evident from the wire tension measurement which failed as well for these tubes), one other had by mistake HV type end-plugs mounted on both sides and, to balance the books, another had S type end-plugs mounted on both sides.

The BOL experience led us to skip this cumbersome test for the BML tubes. (In fact we felt we should have ran a simply HV check in air, but we did not get around doing this!)

5 Summary

- **Components:** The components as used by us will certainly evolve significantly in

the years to come. Clearly component dimensions, like end-plug and wire locator outer diameters, must be investigated. A wire locator consisting of two symmetric halves is probably an excellent idea. Regarding the end-plug: we think it would be wise to rely for the gas seal only on O-rings and not on glue. Also azimuthal symmetry, like the Pavia end-plug, is a nice feature even though preliminary tube assembly experience shows that a lack of azimuthal symmetry, like the Frascati end-plug, is not problematic. We think the wire must be checked to some extent (diameter, defects) prior to wiring. The wire crimp is certainly going to be a hotly debated issue in the coming year!

- **Assembly:** The wiring setup at CERN has a long, and perhaps not always successful, history. However, the experience with the wiring of the 285 BML tubes in a semi-automatic fashion looks promising. It for one showed that a single person can wire a tube with a central wire locator in about 5 minutes. This is important, since most of us now accept that the MDT wiring will be a major part of the work required to realize the MDT part of the muon spectrometer. We therefore consider the core of the CERN wiring philosophy, i.e. (semi-)automatic wiring of MDT tubes, an approach to pursue. This means we think in particular end-plug and wire locator re-designs should try to remain (or become) compatible with (or even facilitate!) the sliding of these components thru a tube (or the sliding of the tube around these components; even that is open for discussion). Less important issues are the crimping technique, the wiring setup at CERN can accommodate any crimping technique, this despite the fact that we were pleased with the air-pressure crimp. An issue which is still in an un-satisfactory state is the wire crimp. We must try hard to find a reliable method which can be automatized. If we succeed the wiring can be performed in an automatic i.e. uniform way; yielding tubes of consistent quality, largely independent of human operators.
- **Quality Control:** We inspected all tubes for the BOL and BML MDT chamber prototypes for wire location, wire tension and leak rate. In addition we verified tube operation of all BOL tubes. As expected, the tube quality assurance turned out to be a time consuming affair. Future wiring efforts should consider at least a partial integration of the wiring proper and the essential tube quality control.

We consider the measurement of the wire tension a routine affair. This, or an alternative method, ought to be integrated into any future wiring setup.

Our helium setup for the determination of the leak rate, with a few modifications to speed up the measurement, looks attractive since it is very precise and measures exactly what the leak rate will be in the real environment. Only disadvantage is that it requires an expensive device. Its integratebility into a wiring setup remains an open question.

The X-ray technology for the measurements of the wire location is nice and precise in principle, however we need to find better ways to position the tube into the X-ray clamp. Also the image registration must be changed from films to CCDs to eliminate the very time consuming task of X-ray film scanning. Moreover, with CCDs the wire location information is available directly. In principle our present setup could easily be integrated into a tube wiring setup. Whether this is desirable in view of safety or whether this is needed in view of the precision remains an open issue.

The verification of tube operation turned out to be very time consuming. This to a very large extent due to the long time it takes to get a proper gas well mixed into a tube. It probably would be wiser to limit this test to a simple high voltage test in air. This also because this test did not yield any surprises; the only 5 tubes which failed the test had either broken wires (3) or wrong end-plugs (2).

5.1 Summary of BOL and BML tube quality

- *Wire tension: we achieved about 2% precision.*
- *Leak rate: we expect leak rates of the order of 10^{-8} Bar \times Litre/Second.*
- *Wire location: we have to study the implications of the poor mount of the tubes in the X-ray jig. This in particular for the central wire locator. If we would ignore the strange phenomena observed in some distributions, we would conclude that both the Italian and the German wire locators can locate wires with a precision of about 20 μm .*
- *Tube operation: we often observed high, order 100 nA, leak currents. Most likely these were due to high humidity. For the prototypes the humidity will be suppressed because of the heat generated by the electronics on the hedgehog printed circuit boards mounted directly on the chambers.*

A Parameters of the produced BOL tubes

Tube Number	Tension g	Leak	Locator	Tubelenght	Deviation μm			
					a	b	c	d
135	262.0		DDD	1	0.006	0.021	0.013	0.028
136	259.5		DDD	1	0.011	0.032	0.024	0.028
137	265.5		DDD	1	0.050	0.018	0.017	0.034
138	262.0		DDD	1	0.010	0.029	0.027	0.044
139	259.0		DDD	1	0.029	0.031	0.026	0.016
140	259.0		DDD	1	0.025	0.045	0.033	0.048
141	260.5		DDD	1	0.035	0.025	0.017	0.036
142	262.0		DDD	1	0.010	0.033	0.022	0.018
143	258.5	LEAK	DDD	1	0.041	0.018	0.018	0.022
144	252.5		DDD	1	0.023	0.015	0.015	0.004
145	260.0	LEAK	DDD	1	0.031	0.038	0.014	0.012
146	0.0	LEAK	DDD	1	0.000	0.000	0.000	0.000
148	259.0		DDD	1	0.011	0.023	0.014	0.040
149	261.0		DDD	1	0.042	0.017	0.027	0.018
150	260.5		DDD	1	0.023	0.013	0.030	0.035
151	263.5		DDD	1	0.024	0.019	0.028	0.027
152	258.0		DDD	1	0.023	0.011	0.085	0.013
153	256.6		DDD	1	0.010	0.046	0.023	0.037
154	257.0		DDD	1	0.013	0.025	0.010	0.016
155	258.0		DDD	1	0.031	0.011	0.004	0.011
156	258.5		DDD	1	0.018	0.057	0.009	0.008
157	256.0		DDD	1	0.019	0.026	0.039	0.015
158	258.0		DDD	1	0.007	0.033	0.039	0.008
159	257.0		DDD	1	0.095	0.011	0.015	0.004
160	260.0		DDD	1	0.052	0.026	0.056	0.046
161	267.5		DDD	1	0.018	0.020	0.024	0.051
162	261.0		DDD	1	0.032	0.018	0.038	0.024
163	263.5		DDD	1	0.018	0.017	0.047	0.012
164	265.5		DDD	1	0.011	0.016	0.016	0.025
165	265.0		DDD	1	0.016	0.036	0.034	0.045
166	269.0		DDD	1	0.022	0.039	0.019	0.013
167	266.0		DDD	1	0.021	0.026	0.005	0.037
169	266.5		DDD	1	0.000	0.000	0.000	0.000
170	263.5		DDD	1	0.003	0.010	0.018	0.007
172	264.0		DDD	1	0.044	0.018	0.005	0.028
173	265.0		DDD	1	0.025	0.016	0.015	0.025
174	264.0		DDD	1	0.022	0.012	0.026	0.024
175	260.5	LEAK	DDD	1	0.015	0.047	0.027	0.023
177	260.5		DDD	1	0.015	0.028	0.051	0.057
178	262.0		DDD	1	0.031	0.055	0.048	0.040
179	259.0		DDD	1	0.032	0.019	0.019	0.039

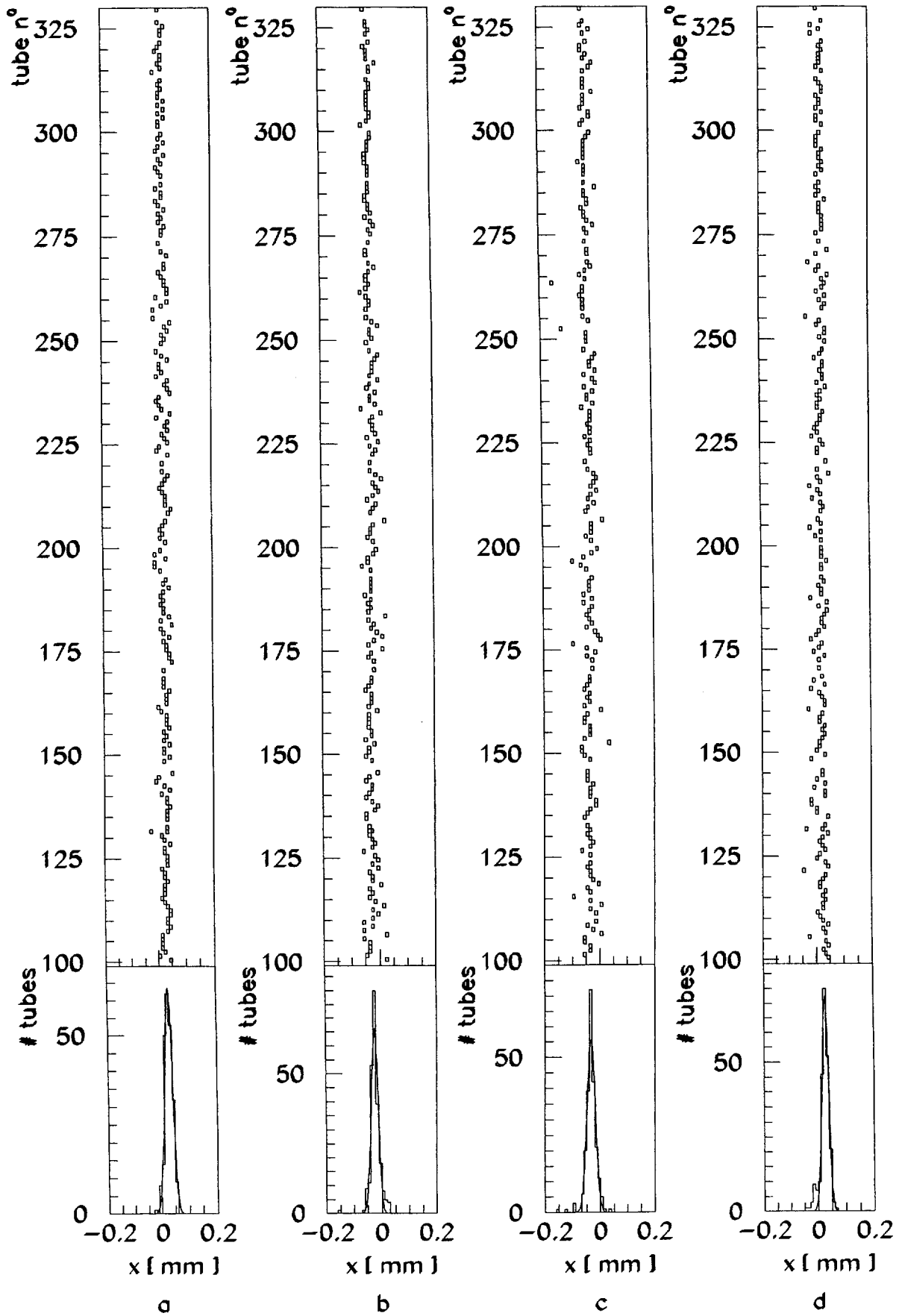


Figure 22: Horizontal wire location BOL tubes; German locator. (a) HV end (b) Signal end (c-d) Central. Note: labels a,b,c,d are used inconsistently. Must be changed to terminology as used in text and BML plots.

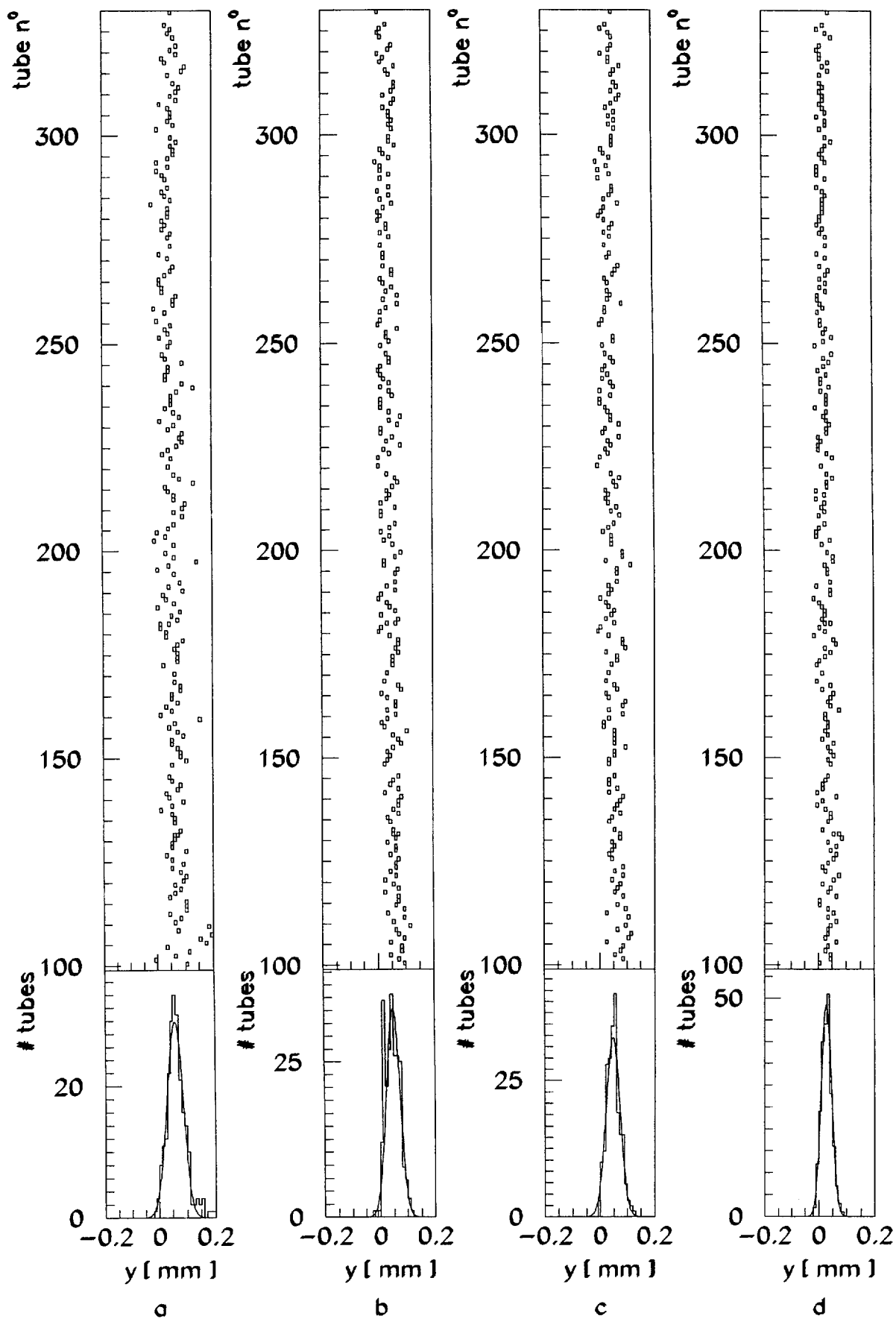


Figure 23: Vertical wire location BOL tubes; German locator. (a) HV end (b) Signal end (c-d) Central. Note: labels a,b,c,d are used inconsistently. Must be changed to terminology as used in text and BML plots.

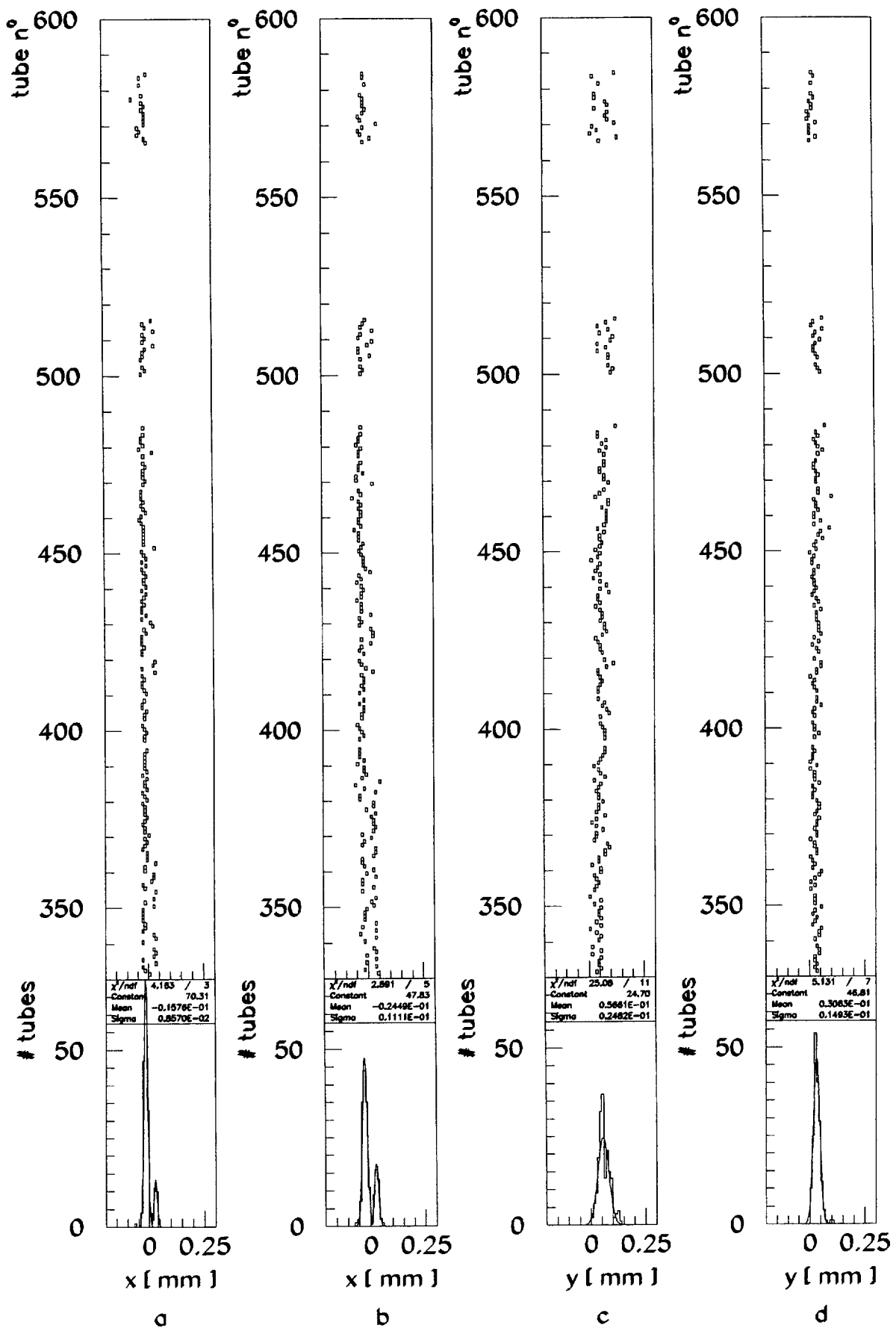


Figure 24: Wire locations BOL tubes; Italian locator. (a) HV end horizontal (b) Signal end horizontal (c) HV end vertical (b) Signal end vertical. Note: labels a,b,c,d are used inconsistently. Must be changed to terminology as used in text and BML plots.

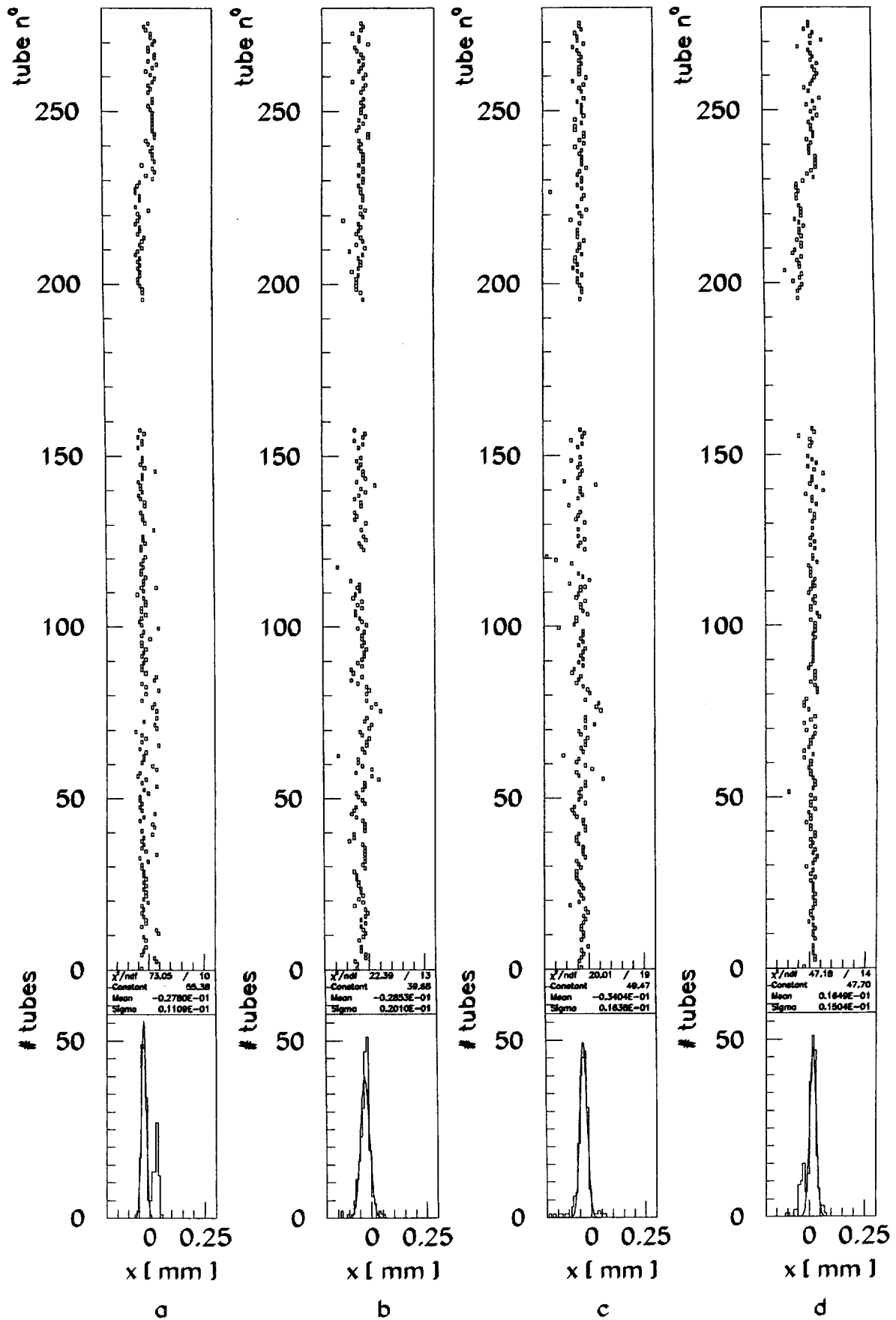


Figure 25: Horizontal wire location BML tubes. The vertical scale shows the sequential number of the tubes and the horizontal scales shows the coordinate in mm. The labels a, b, c and d refer to the locations of the wire locators: a and b are at tube ends and b and c are on the two sides of the central wire locator.

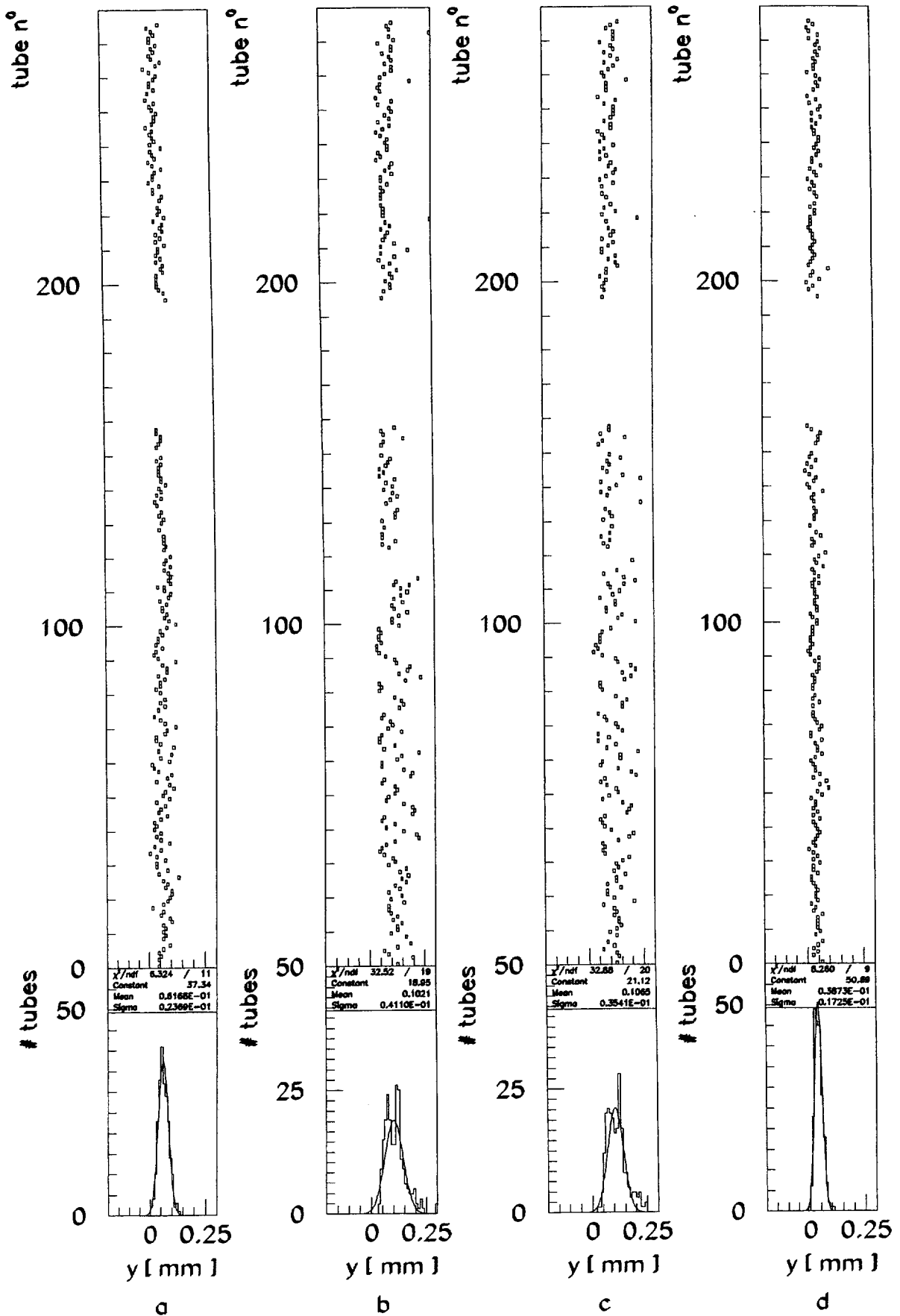


Figure 26: Vertical wire location BML tubes. The vertical scale shows the sequential number of the tubes and the horizontal scales shows the coordinate in mm. The labels a, b, c and d refer to the locations of the wire locators: a and b are at tube ends and b and c are on the two sides of the central wire locator.

February 28, 1996

**Wire Positions
in
Monitored Drift Tubes**

ATLAS
A.P. Colijn and F. Linde

Abstract

Anode wire positions in Monitored Drift Tubes have been measured making use of a stereo Rontgen-picture technique. The measurement has been done to test the accuracy of the wire fixation inside the tubes.

1 Introduction

To measure wire positions inside an MDT tube a stereo-picture technique is used; two X-ray cameras simultaneously take a picture of the same tube under different angles. The MDT tube is fixed inside a calibration setup, which consists of wires (reference wires) which are placed in well defined positions parallel to the wire inside the tube. If the X-ray pictures are then taken through the tube, on both pictures five lines are seen. From the relative positions of the five lines the geometry of the calibration setup as well as the position of the wire inside the tube can be solved.

2 Principle of Measurement

A schematic view of the setup used to take the X-ray pictures is shown in figure 1a. X-ray source 1 (2), reference wire planes $d11$ and $d12$ ($d21$ and $d22$), together with film 1 (2) define the local coordinate system 1 (2), which will be referred to as station 1 (2). Figure 1b shows

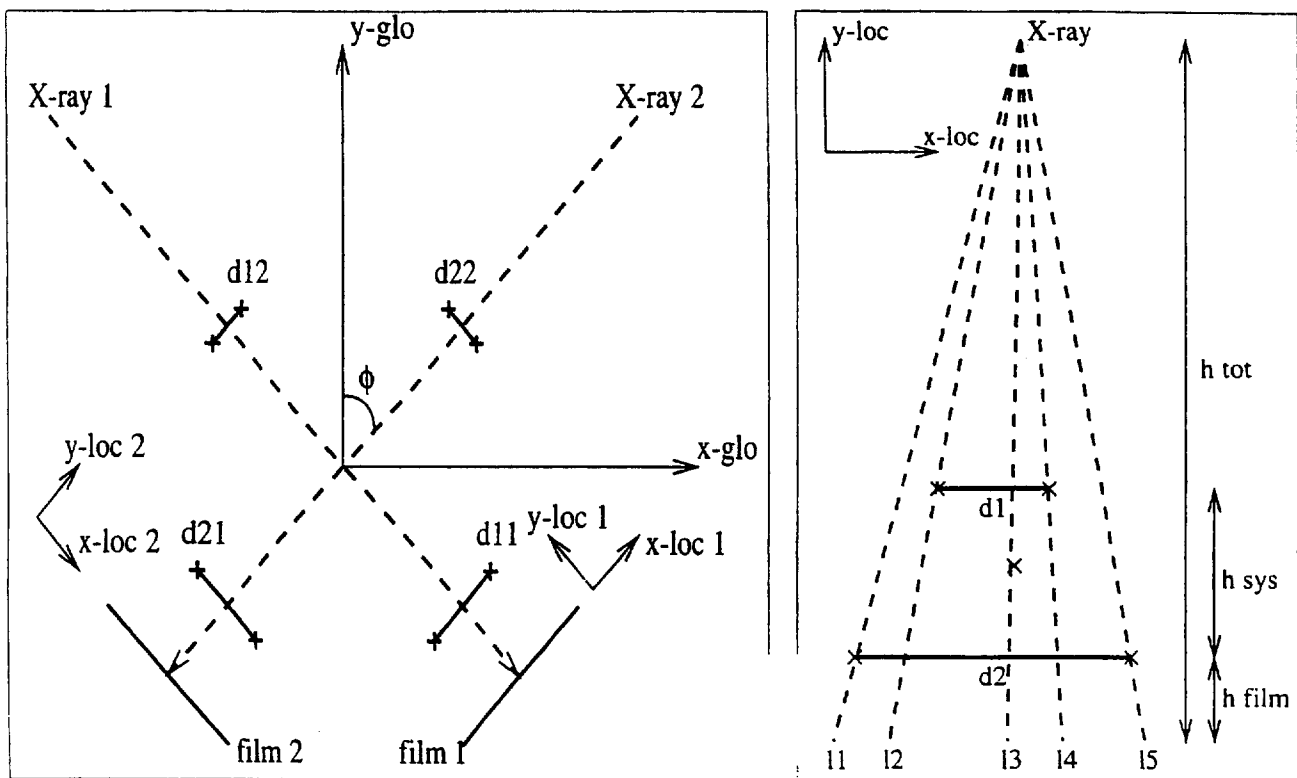


Figure 1: Schematic view of the setup used for taking the stereo-pictures of the MDT tubes (a). The definitions of the global and local coordinate frames are shown. The small crosses indicate the positions of the reference wires. In (b) the definitions in one of the two local frames are shown.

the geometrical definitions in one of the stations. The parameters $l1, \dots, l5$ are the x -positions of the wires as seen on the X-ray picture; $l1, l2, l4$ and $l5$ are the images of the reference wires and $l3$ is the position of the wire to determine the position of (probe wire).

Solving the position of the probe wire is basically done in three steps. First the geometry of both the stations has to be solved. Then in both the stations an equation of the form

$x_{wire} = ay_{wire} + b$ for the wire position is found. The third step is to find the intersection of both lines in the global coordinate frame, thus giving the probe wire position.

The geometry can be solved in the assumption h_{sys} , $d1$ and $d2$ are known and that the wire planes are centered around $x = 0$ in the local coordinate frame. Also all reference wires as well as the probe wires are supposed to be strung parallel in the plane perpendicular to figure 1. First the heights h_{film} and h_{tot} can be solved from the magnification of the sizes $d1$ and $d2$. The following can be derived for the y -position of the film:

$$h_{film} = h_{sys} \cdot \left(1 - \frac{d1}{l_{15}}\right) / \left(\frac{d1}{l_{15}} - \frac{d2}{l_{24}}\right) \quad (1)$$

and for the distance between the film and the $X - ray$ source:

$$h_{tot} = h_{sys} / \left(\frac{d1}{l_{15}} - \frac{d2}{l_{24}}\right) \quad (2)$$

In these equations l_{ij} indicates the distance between line i and line j on the $X - ray$ image. If one assumes both the wire planes $d1$ and $d2$ to be symmetric around $x = 0$, then the x -position of the $X - ray$ source can be solved as a function of l_{12} and l_{45} . The following expression can be derived:

$$x_{X-ray} = (l_{12} - l_{45}) / 2 \cdot (\rho - \sigma) \quad (3)$$

where

$$\rho = \frac{h_{tot}}{h_{tot} - h_{film}} \quad \text{and} \quad \sigma = \frac{h_{tot}}{h_{tot} - h_{film} - h_{sys}} \quad (4)$$

The distances of the projections of the lower reference wires to the projection of the probe wire can be used to derive a first order equation for the wire position in the local coordinate frame:

$$x_w^{loc} = a_{sys}^{loc} \cdot y_w^{loc} + b_{sys}^{loc} \quad (5)$$

with

$$a_{sys}^{loc} = \frac{l_{35} - l_{13}}{2h_{tot}} + \frac{x_{X-ray}}{h_{tot} - h_{film}} \quad \text{and} \quad b_{sys}^{loc} = -h_{tot} \cdot a_{sys}^{loc} \quad (6)$$

After the geometry is solved and the equation for the probe wire position has been calculated for both the stations, the next step is to transfer the two linear equations to the global coordinate frame and to find the intersection. In the global coordinate frame the two stations intersect halfway the two reference wire planes. The angle of the local y -axis with the global one for station 1 (2) is called ϕ_1 (ϕ_2). The origin of the global coordinate frame is set at the intersection point of the axes of the two stations (the dashed lines in figure 1). After the coordinate transformation equation 6 can be written as:

$$x_w^{glo}(k) = y_w^{glo}(k) \cdot A(k) + B(k) \quad (7)$$

with

$$A(k) = \frac{\sin \phi_k + a_{sys}^{loc} k \cos \phi_k}{\cos \phi_k - a_{sys}^{loc} k \sin \phi_k} \quad \text{and} \quad B(k) = \frac{\gamma_k a_{sys}^{loc} k + b_{sys}^{loc} k}{\cos \phi_k - a_{sys}^{loc} k \sin \phi_k} \quad (8)$$

where the extra index k runs from 1 to 2 to describe both the stations and γ_k is the local y coordinate of the intersection.

Then remains the simple solution to the intersection, which yields:

$$\begin{cases} x_{wire} = \frac{A(1)B(2) - A(2)B(1)}{A(1) - A(2)} \\ y_{wire} = \frac{B(2) - B(1)}{A(1) - A(2)} \end{cases} \quad (9)$$

3 Calibration

Before wire positions in real tubes can be calculated, possible offsets in the x_{wire} and y_{wire} coordinates have to be taken into account. Therefore a calibration run is performed, rotating a tube with a well defined circular surface and taking pictures under different angles. The positions of the probe wire will describe a circle in the (x, y) plane, from which basically two quantities can be measured. The first is the displacement of the wire from the center of the tube, which is given by the radius of the circle. The second one are the x and y offsets, which are directly given by the x and y coordinates of the center of the circle.

The fitting procedure is as described in the previous section and the values for the fixed parameters are listed in table 1. The calibration run is performed, by taking stereo pictures

	station 1	station 2
$d1$	3.99 mm	3.99 mm
$d2$	2.09 mm	2.07 mm
h_{sys}	72.9 mm	76.0 mm
ϕ	-52.5°	52.5°

Table 1: Geometry constants for both station 1 and 2.

under 12 different angles from 0° to 360° with steps of 30° . Figure 2 shows the reconstructed points in the (x, y) plane. The circle is fitted through the points using a fitting method developed by Karimaki (ref). The radius of the circle / wire displacement is $11.7\mu m$ and the offsets in x and y are $-16\mu m$ and $-3\mu m$ respectively. The residuals in r are shown in figure 3. An indication of the accuracy of the measurement is given by the RMS of the distribution, which is $3.5\mu m$.

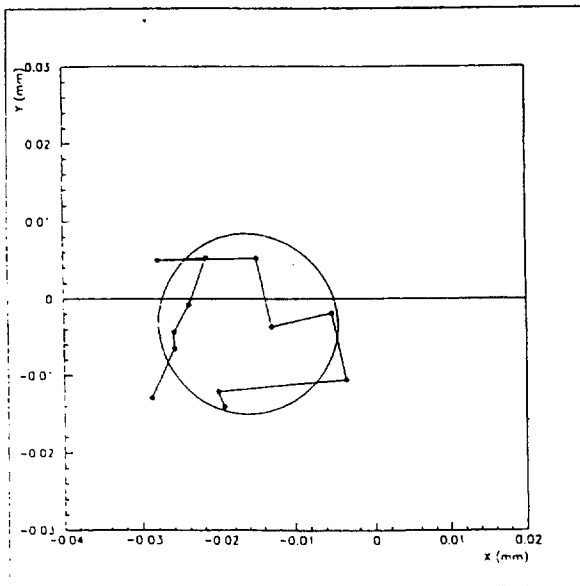


Figure 2: Scatter plot of the reconstructed wire coordinates x_{wire} and y_{wire} .

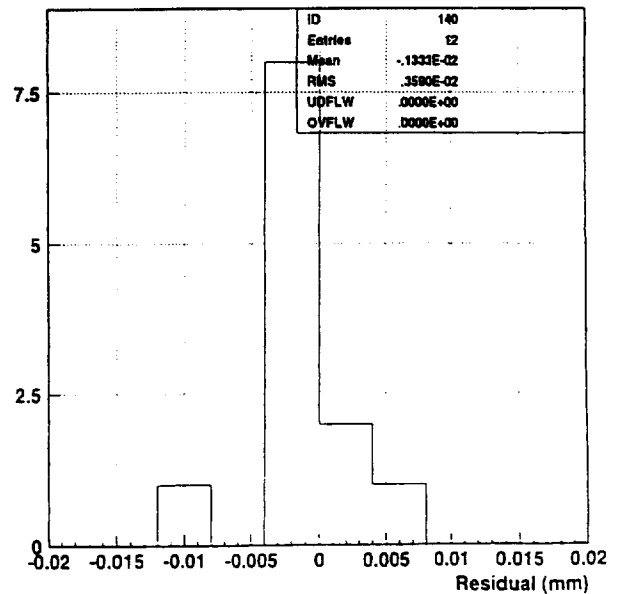


Figure 3: Distance of the fitted circle to the measured points of the calibration run.

4 Measurement on real tubes

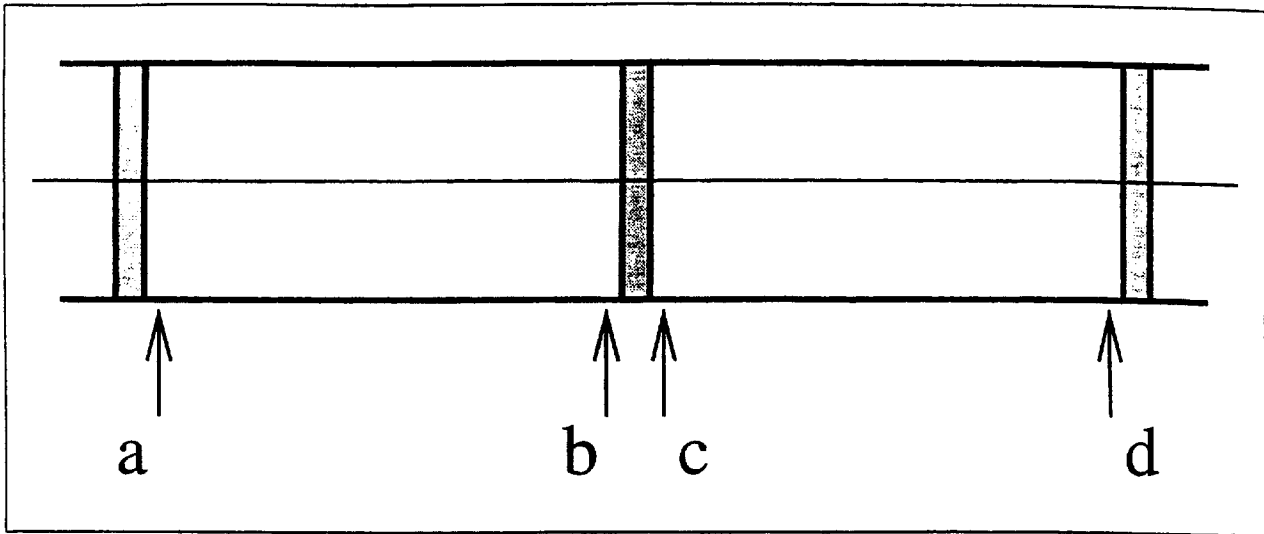


Figure 4: *The position of the wire in the tube is determined at the wire locator positions, which are indicated with a,...,d*

After the offset calibration, X-ray scans of "real" tubes are performed. The tubes scanned have 3 wire locators; two at both ends and one in the center of the tube (see figure 4). At positions a, b, c and d the position of the wire is determined.

Table 2 shows the positions of the wires inside the 15 tubes that have been scanned, without the offset subtraction of $x = -16\mu m$ and $y = -3\mu m$. The positions of the wires are graphically displayed in figure 5. The average x position is $-14\mu m$ and the average y position is $4\mu m$, which is in good agreement with the offsets obtained from the calibration, especially if one takes into account that now 'real' misplaced wires are used to calculate the offset. After offset subtraction the absolute wire displacement is calculated for wire positions b and c. The resultant distribution of displacements is shown in figure 6 and the corresponding values are listed in table 3. The average wire displacement is $(32 \pm 27\mu m)$.

In order to check the consistency of the measurements, for the first three tubes the measurement of the line positions on the X-ray pictures have been repeated three times (indicated a,b, c in table 2. The three different measurements show deviations in the order of $10\mu m$. Moreover the whole measurement for all tubes has been repeated, to check the reproducibility of the X-ray pictures themselves. The positions of the wires at the central wire locator can be reproduced within about $10\mu m$. The reproduction of the wire positions at the end locators is much worse, which can be explained from the fact that the positioning of the tubes inside the reference block is harder for those positions.

Another consistency check is done by performing calibration runs, but now on 'real' tubes. For this purpose tube 1 at position b is photographed under 12 different angles. A circle fit gives a wire displacement of $42\mu m$, which is comparable with the $45\mu m$ found before. Also the offsets (see section 3) reproduce very well; the offsets are now found to be $(-8, -4)$. Moreover, a detailed calibration run of tube 1 b has been performed to get an accurate description of the x and y offset behaviour.

Figure 7 shows the x and y positions for photographs taken under 16 different angles. An effort is done to see if the tubes are elliptical. For this purpose the following function is fit to

tube	a	b	c	d	Remarks
1 Ia standard	-70, -20	-3, 40	-2, 50	-18, 2	
1 Ib	-65, -21	-3, 40	-6, 42	-14, 7	
1 Ic	-67, -17	-0, 42	-4, 45	-16, 12	
1 IIa	-61, -7	-6, 38	-4, 50	-14, 23	
2 Ia standard	-202, 2	-14, -4	4, 56	2, -73	note very bad position a
2 Ib	-21, 17	-19, -12	-5, 50	9, -75	
2 Ic	-21, 17	-14, -14	-6, 55	2, -71	
2 IIa	-210, 17	-22, -20	-5, 60	30, -40	
3 Ia standard	-21, 17	3, -8	-25, 11	5, 5	
3 Ib	-25, 20	4, -13	-21, 8	8, -2	
3 Ic	-30, 18	15, -7	-21, 6	8, 1	
3 IIa	-9, 63	10, -18	-27, 13	-2, -40	
4 Ia teflon no crimp	—	—	—	—	
4 IIa	45, 66	23, 53	21, 47	21, 48	
5 Ia teflon no crimp	-52, -4	-42, -25	-47, -22	-94, 49	
5 IIa	-47, -11	-48, -17	-36, -10	-93, 74	
6 Ia teflon no crimp	18, -16	13, 1	25, 10	-37, 1	
6 IIa	-6, 54	15, 6	42, 12	-25, -23	
7 Ia standard	-23, -15	-17, -1	-18, -4	-8, -15	
7 IIa	-22, -10	-20, 9	-15, 1	1, -16	
8 Ia standard	39, -22	-2, -11	0, -11	-11, -9	
8 IIa	17, 27	-1, -4	-1, -15	-23, -1	
9 Ia standard	—	-8, -13,	-67, 50	-23, 7	kink in wire position in middle locator
9 IIa	—	2, -25	-75, 54	-16, -5	
10 Ia teflon crimp	19, -9	-114, -37	67, 38	63, 53	kink in wire position in middle locator
10 IIa	7, -1	-112, -76	47, 35	31, 44	
11 Ia teflon crimp	-5, -4	-13, -7	-10, 1	-38, 29	
11 IIa	7, -7	-13, -5	-16, 1	-27, -1	
12 Ia teflon crimp	47, 37	-10, -25	-44, -23	-17, 49	
12 IIa	41, 27	-16, -18	-41, -23	-17, 57	
13 Ia	2, 26	-16, 3	-21, 9	-29, -32	
14 Ia	-15, -12	-17, -4	-21, -6	-5, 1	
15 Ia	-15, 5	-30, -27	-28, -34	-24, -60	

Table 2: Wire positions of the test tubes, without the subtraction of the offset. Ia, Ib and Ic indicate the results of different scans to the same pictures. IIa is obtained from a different set of pictures.

x and y :

$$\begin{cases} x = a_1 \cos(\phi - \phi_1) & + b_1 \cos 2(\phi - \phi_2) \\ y = a_1 \cos(\phi - \phi_1 - \frac{\pi}{2}) & + b_2 \cos 2(\phi - \phi_2 - \phi_3) \end{cases} \quad (10)$$

The first term in both the equations are due to the displacement of the wire and the second term describes the wire position due to a non circular tube. In figure 7 the solid curve represents the result of a simultaneous fit to x and y . For the fit errors of $10 \mu m$ for both x and y are assigned. The wire displacement is found to be $29 \mu m$, the amplitudes due to the ellipticity(?) b_1 and b_2 are found to be $-21 \mu m$ and $-15 \mu m$ respectively and the phase difference between the elliptical term in x and y , ϕ_3 is found to be 2.18 rad. These values are (not) consistent with a 'jig' of xxx° . Figure 8 shows x versus y , with superimposed the results of the fit.

A final consistency check is done by taking pictures of 7b and 10c with on one picture the image of the tube under different angles. The 7b picture shows all the images of the wire on top of each other, which corresponds to a zero displacement of the wire (7b after subtraction

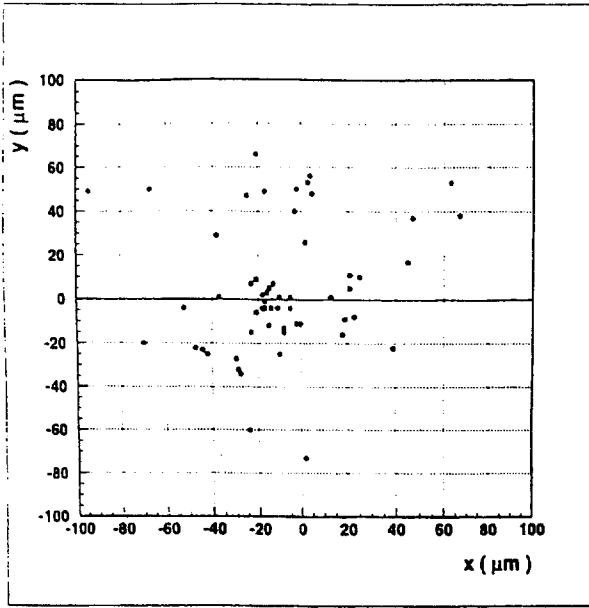


Figure 5: Scatter plot of the reconstructed wire coordinates x_{wire} and y_{wire} . Note that the extremely misplaced wires are not displayed.

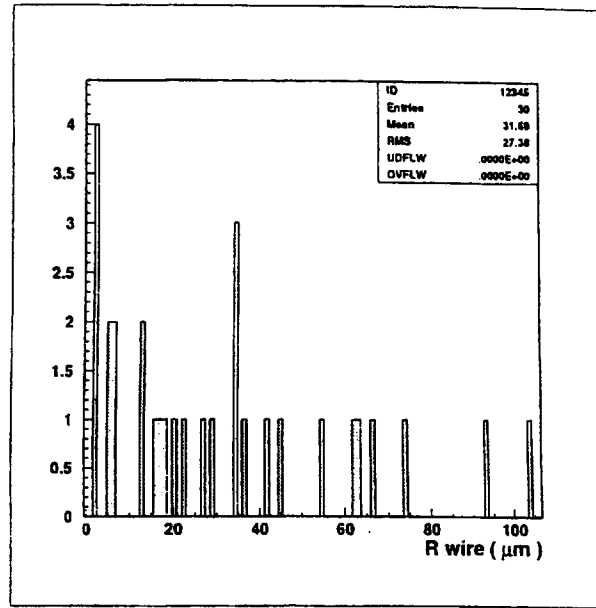


Figure 6: Absolute values of the wire displacements at positions b and c

tube	1	2	3	4	5	6	7	8	9	10	11	12	13	14	15
b	45	2	20	66	34	29	2	16	13	104	5	23	6	2	27
c	55	62	17	83	36	42	2	18	74	93	6	34	13	5	34

Table 3: Wire displacements at positions b and c .

of offsets should have zero offset). The 10c picture shows a separation of the wires of $\approx 200\mu m$ from which an estimate of the wire displacement of $\approx 100\mu m$ can be obtained, which is in reasonable agreement with the $80\mu m$ that is measured in the standard way.

5 Conclusion

The rather large wire displacements of most of the wires can have several explanations. From the previous section the following causes for the wire displacements can be ruled out:

- The scanning of the pictures
- The pictures themselves
- The program to analyze the pictures

This leaves the following possibilities for the bad wire positions:

- The tubes are elliptically shaped, which means the determination of the wire positions cannot be done from one pair of pictures. This effect has been proven present in the previous section. (study in progress)

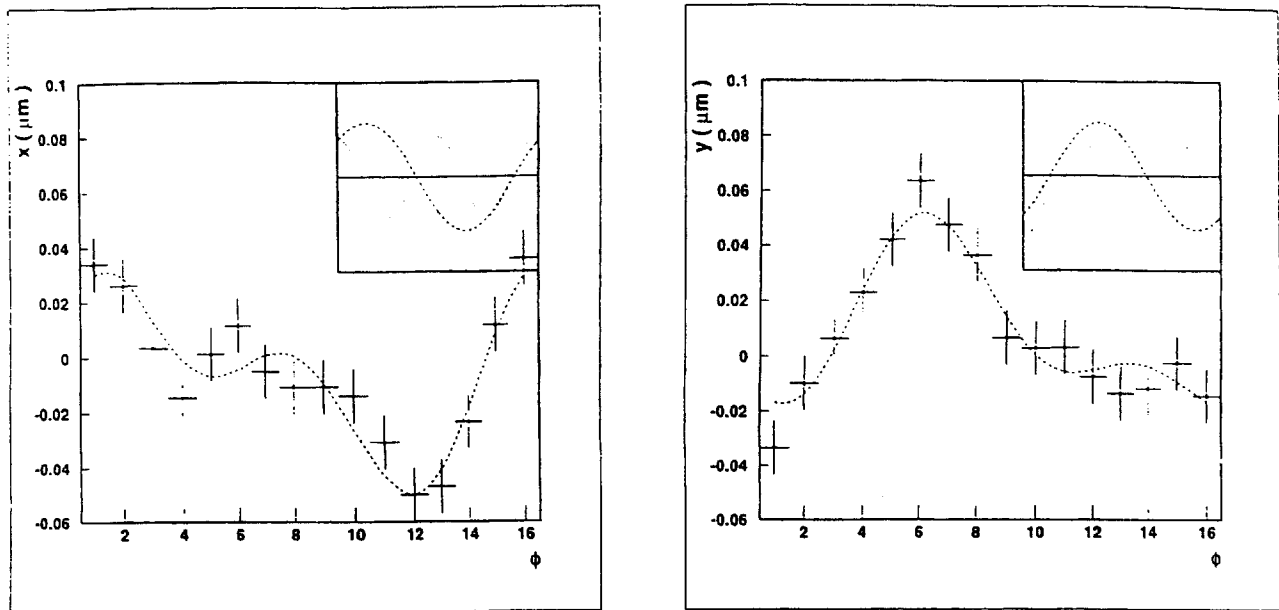


Figure 7: x_{wire} (left) and y_{wire} (right) of tube 1 at position b plotted versus ϕ . The dashed curve is the result of the fit. In the upper right corner of both the plots the $\cos \phi$ and the $\cos 2\phi$ terms from the fit are plotted separately.

- The wires are not well strung in the tubes.
- The wires are really placed off-center in the tubes.

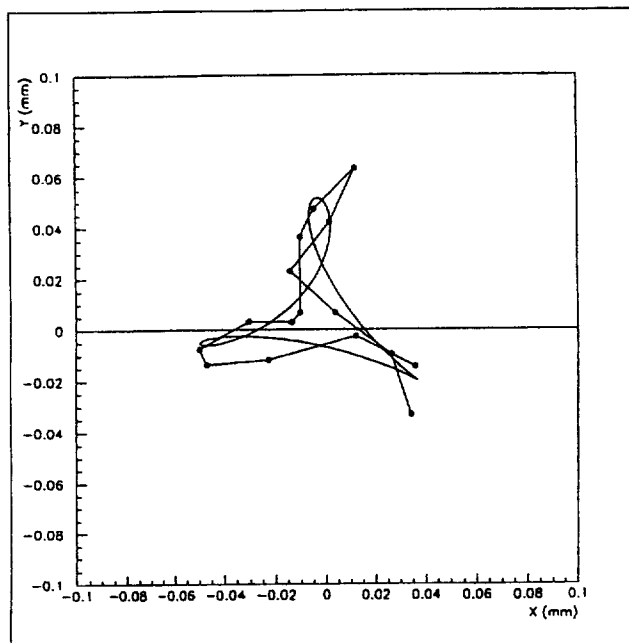


Figure 8: y_{wire} plotted versus x_{wire} . The solid line is the result of the fit.